Assessment of systemic AAV-microdystrophin gene therapy in the GRMD model of Duchenne muscular dystrophy

Sharla M. Birch[1†], Michael W. Lawlor[2‡], Thomas J. Conlon[3], Lee-Jae Guo[1§], Julie M. Crudele[4], Eleanor C. Hawkins[5], Peter P. Nghiem[1], Mihye Ahn[6‖], Hui Meng[2¶], Margaret J. Beatka[2#], Brittany A. Fickau[2], Juan C. Prieto[7], Martin A. Styner[7], Michael J. Struharik[8**], Courtney Shanks[8††], Kristy J. Brown[8], Diane Golebiowski[8‡‡], Amanda K. Bettis[1], Cynthia J. Balog-Alvarez[1], Nathalie Clement[3§§], Kirsten E. Coleman[3], Manuela Corti[3], Xiufang Pan[9], Stephen D. Hauschka[4], J. Patrick Gonzalez[8], Carl A. Morris[8], Joel S. Schneider[8‖‖], Dongsheng Duan[9], Jeffrey S. Chamberlain[4], Barry J. Byrne[3*], Joe. N. Kornegay[1*]

Duchenne muscular dystrophy (DMD) is a progressive muscle wasting disease caused by the absence of dystrophin, a membrane-stabilizing protein encoded by the *DMD* gene. Although mouse models of DMD provide insight into the potential of a corrective therapy, data from genetically homologous large animals, such as the dystrophin-deficient golden retriever muscular dystrophy (GRMD) model, may more readily translate to humans. To evaluate the clinical translatability of an adeno-associated virus serotype 9 vector (AAV9)–microdystrophin (μDys5) construct, we performed a blinded, placebo-controlled study in which 12 GRMD dogs were divided among four dose groups [control, 1×10^{13} vector genomes per kilogram (vg/kg), 1×10^{14} vg/kg, and 2×10^{14} vg/kg; $n = 3$ each], treated intravenously at 3 months of age with a canine codon-optimized microdystrophin construct, rAAV9-CK8e-c-μDys5, and followed for 90 days after dosing. All dogs received prednisone (1 milligram/kilogram) for a total of 5 weeks from day −7 through day 28. We observed dose-dependent increases in tissue vector genome copy numbers; μDys5 protein in multiple appendicular muscles, the diaphragm, and heart; limb and respiratory muscle functional improvement; and reduction of histopathologic lesions. As expected, given that a truncated dystrophin protein was generated, phenotypic test results and histopathologic lesions did not fully normalize. All administrations were well tolerated, and adverse events were not seen. These data suggest that systemically administered AAV-microdystrophin may be dosed safely and could provide therapeutic benefit for patients with DMD.

INTRODUCTION

Duchenne muscular dystrophy (DMD) is an X-linked recessive disorder affecting about 1 in 5000 newborn human males in whom the absence of the protein dystrophin causes progressive degeneration of skeletal and cardiac muscle (*1*). There has been particular interest in potentially corrective genetic therapies, including dystrophin transgene delivery using viral vectors. Gene therapy in DMD has been complicated by two major factors, the limited carrying capacity of conventional viral vectors (*2*) and the potential for an immune response to the viral construct (*3*).

The *DMD* gene transcript is about 14 kb, well exceeding the capacity of the first-generation adenovirus (about 8.2 kb) and adeno-associated virus (AAV, about 4.7 kb) vectors (*4*). To overcome this size limitation, shortened dystrophin transgenes that retain the key elements necessary for protein function have been developed (*5*). The therapeutic potential of these miniaturized genes was predicated on the fact that some sizeable in-frame *DMD* gene deletions cause a much less severe syndrome known as Becker's muscular dystrophy (BMD) (*6*). After encouraging results from muscular dystrophy X-linked (mdx) mice treated intramuscularly with AAV-

[1]Texas A&M University, College of Veterinary Medicine and Biomedical Sciences, College Station, TX 77843, USA. [2]Medical College of Wisconsin, Milwaukee, WI 53226, USA. [3]Powell Gene Therapy Center, University of Florida, Gainesville, FL 32610, USA. [4]University of Washington, Seattle, WA 98109, USA. [5]College of Veterinary Medicine, North Carolina State University, Raleigh, NC 27606, USA. [6]University of Nevada-Reno, Reno, NV 89557, USA. [7]University of North Carolina, Chapel Hill, NC 27599, USA. [8]Solid Biosciences Inc., Cambridge, MA 02142, USA. [9]School of Medicine, University of Missouri, Columbia, MO 65212, USA.
†Present address: Lovelace Biomedical, Albuquerque, NM 87108, USA.
‡Present address: Diverge Translational Science Laboratory, Milwaukee, WI 53204, USA.
§Present address: CBSET Inc., Lexington, MA 02421, USA.
‖Present address: University of Nevada-Reno, Reno, NV 89557, USA.
¶Present address: Diverge Translational Science Laboratory, Milwaukee, WI 53204, USA.
#Present address: Diverge Translational Science Laboratory, Milwaukee, WI 53204, USA.
**Present address: Biogen, Cambridge, MA 02142, USA.
††Present address: Decibel Therapeutics Inc., Boston, MA 02215, USA.
‡‡Present address: Oxford Biomedica Solutions, Bedford, MA 01730, USA.
§§Present address: Unicorn Consultations, Gainesville, FL 32608, USA.
‖‖Present address: Carbon Biosciences, Boston, MA 02199, USA.
*Corresponding author. Email: joenkornegay@gmail.com (J.N.K.); barry.byrne@ufl.edu (B.J.B.)

microdystrophin constructs (*7*, *8*), a small DMD clinical trial was conducted (*9*, *10*). Although evidence of dystrophin production was observed, a T lymphocyte response was noted to the transgene protein and preexisting dystrophin epitopes (*9*) with interferon-γ enzyme-linked immunosorbent spot (ELISPOT) assays.

Studies had been done on a somewhat delayed basis in a genetically homologous canine disease originally characterized in golden retriever dogs and termed either canine X-linked muscular dystrophy (CXMD) or golden retriever muscular dystrophy (GRMD) (*11*). Dystrophic dogs treated by intramuscular injection of AAV-microdystrophin constructs showed a marked immune response to either the transgene protein (*12*) or AAV capsids (*13*), although ELISPOT assays were not done. In both the canine studies and human trial, a ubiquitous cytomegalovirus (CMV) promoter was used, with the potential for greater gene expression in nonmuscle tissues and an associated immune response. Subsequent studies showed that persistent microdystrophin expression could be achieved after intramuscular injection of AAV constructs with a CMV promoter if dogs were immunosuppressed (*14*, *15*). To reduce the immune response to the microdystrophin protein, muscle-specific regulatory cassettes (*16*) that restrict expression to skeletal and cardiac muscle have been increasingly used (*17*). Providing proof of concept, a single dystrophic dog treated with a microdystrophin construct that included a muscle-specific promoter showed dystrophin expression for 8 weeks without immunosuppression (*18*).

Localized gene therapy has been seen as the first step toward systemic administration and associated body-wide effects. Intravascular delivery may be less immunogenic, given that side effects of intramuscular injection likely occur partly due to tissue injury and the concentrated antigen load (*19*). Consistent with this point, systemic administration of AAV-microdystrophin constructs achieved widespread dystrophin expression and, in some cases, improved skeletal muscle and/or cardiac function in mdx mice (*20*–*22*) and dystrophic dogs (*23*, *24*) without a substantial immune response.

Here, we report data from a blinded, placebo-controlled study in which GRMD dogs were treated intravenously with a single dose of an AAV9 vector carrying a codon-optimized, canine version of the microdystrophin-5 (μDys5) complementary DNA. The μDys5 transgene encodes a functionally enhanced microdystrophin that includes the localization domain for neuronal nitric oxide synthase (nNOS) (*4*, *17*). A human version of μDys5 being used in the Solid Biosciences (SGT-001) clinical trial (https://clinicaltrials.gov/ct2/show/NCT03368742) is distinct from earlier-generation microdystrophins used in other ongoing trials (*4*). We observed dose-

A

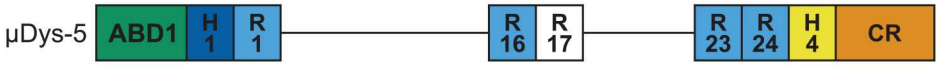

B

Group	Test article or control/vehicle	Dose level (vg/kg)	Animals	Sex
Low dose	rAAV9-CK8-c-μD5	1×10^{13}	Paulie	Male
			Revolver	Female
			Red	Female
Mid dose	rAAV9-CK8-c-μD5	1×10^{14}	Sylvio	Male
			Goldspot	Female
			Frank	Male
High dose	rAAV9-CK8-c-μD5	2×10^{14}	Ladybug	Female
			Zeigan	Male
			Pikachu	Female
Vehicle	1× PBS	0	Tony	Male
			Babydoll	Female
			Charmander	Male

C

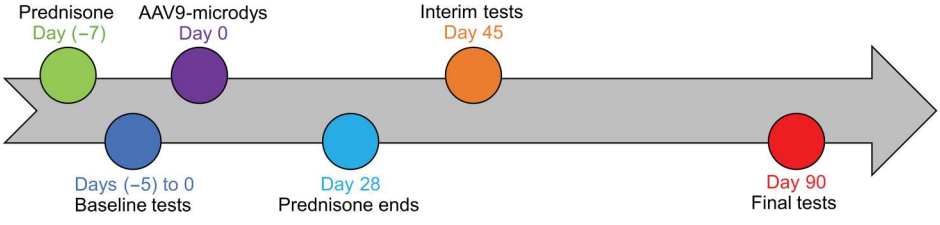

Fig. 1. Experimental design and timeline for AAV9-microdystrophin injection in GRMD dogs. (**A**) An AAV9 construct containing a microdystrophin (μDys5) consisting of the N-terminal actin-binding domain (ABD1), two hinges (H1 and H4), five spectrin-like repeats (R1, R16, R17, R23, and R24), and the cysteine-rich (CR) domain with the muscle-specific CK8e expression cassette was injected. (**B**) Dogs were randomly assigned to one of four groups ($n = 3$ for each) that received a single intravenous dose of the AAV9-μDys5 or vehicle based on the dose of AAV9 received: group 1: 1×10^{13} vg/kg, low dose; group 2: 1×10^{14} vg/kg, mid dose; group 3: 2×10^{14} vg/kg, high dose; and group 4: 0 vg/kg, vehicle (control). (**C**) AAV9-μDys5 was administered on day 0 (baseline) when dogs were about 90 ± 10 days (3 months) of age. Prednisone (1 mg/kg orally) was begun 7 days before AAV9-μDys5 injection and continued without tapering the dose for a total of 35 days. Anti-AAV9 circulating antibodies were measured at baseline and on several subsequent days until termination at about study day 90. Phenotypic testing was done within 5 days before AAV9-μDys5 injection and then repeated on days 45 and 90 (about 4.5 and 6 months of age), each ±5 days to accommodate scheduling the various tests.

dependent increases in tissue vector genome copy numbers and improvement in several functional and pathologic outcomes in treated dogs. These results support the potential value of systemic AAV-microdystrophin to treat patients with DMD.

RESULTS

A single infusion of rAAV9-CK8e-c-μDys5 or vehicle was administered intravenously at increasing doses into four groups of GRMD dogs using a 3-month experimental timeline

We used a construct containing the canine codon-optimized version of the microdystrophin μDys5 transgene, rAAV9-creatine kinase 8 (CK8e)-c-μDys5 (Fig. 1A) (*25*), to lessen the potential immunogenicity of a human transgene being expressed in dogs (*26*, *27*). A dose escalation study was devised using doses that largely paralleled the 1.5×10^{13} to 6.23×10^{14} vector genomes per kilogram (vg/kg) range previously used in GRMD microdystrophin studies (*23*, *24*, *26*). Dogs were randomly assigned to one of four treatment groups ($n = 3$ for each) that received a single intravenous dose of the rAAV9-CK8e-c-μDys5 construct or vehicle: group 1: 1×10^{13} vg/kg, low dose; group 2: 1×10^{14} vg/kg, mid dose; group 3: 2×10^{14} vg/kg, high dose; and group 4: 0 vg/kg, vehicle (control) (Fig. 1B). We expected to see a clear dose response with the 10-fold increase between the low- and mid-dose groups and a further incremental increase by doubling the middle dose to the high dose. A standard 3-month timeline was used, performing baseline and terminal studies at 3 and 6 months of age (*11*).

To lessen the potential immune response, we gave prednisone (1 mg/kg) orally to all GRMD dogs for 5 weeks, without tapering the dose, starting on day −7 and ending on day 28 (Fig. 1C). Diphenhydramine was administered subcutaneously (2 mg/kg) 30 min before dosing to decrease the likelihood of a hypersensitivity response, as we have done previously when administering proteins to GRMD dogs (*28*).

All GRMD dogs were determined to be seronegative for AAV9 at 90 ± 10 days (~3 months) of age (day 0; baseline). Anti-AAV9 circulating antibodies were measured on several subsequent days until termination at about study day 90 (table S1). Baseline phenotypic testing was done within 5 days before the AAV9-μDys5 injection and then repeated for all tests but MRI on days 45 and 90 (about 4.5 and 6 months of age), each ±5 days to accommodate scheduling the various tests. MRI was performed only at baseline and day 90. In assessing all findings, we were mindful of the well-established tendency for phenotypic variation in GRMD, whereby functional and pathologic findings vary among affected dogs (*29*). For functional studies, therapeutic efficacy was best shown by calculating the percent difference between baseline and posttreatment values, allowing each dog to essentially serve as its own control.

Dose-dependent AAV9 vector DNA was evident in body fluids and stool by day 7 and then tapered

Blood sample vg copies/μg genomic DNA (gDNA) group means were below the positive cutoff (>100 vg copies/μg gDNA) at baseline (fig. S1A), except for the high-dose group that had a mean positive value of 6685 vg/μg gDNA. This reflected a markedly elevated value of 18,250 vg/μg gDNA in a single dog that likely occurred because all dogs were closely housed, potentially allowing body fluids to be shared. Group means in all dose groups were positive at day 7 after injection and subsequently decreased at day 16. A small increase occurred from days 16 to 31 in the low- and mid-dose groups, followed by a continual decrease from days 31 to 90. Mean concentrations from vehicle-injected control dogs remained below the positive cutoff at each time point (fig. S1A).

We assessed viral shedding in treated dogs using a positive cutoff of >100 vg copies/μg gDNA. Nasal swabs showed dose-dependent increases at day 7 (fig. S1B). A continuous decrease from days 7 to 90 was observed in each of the three dose groups. By day 90, all groups remained positive in a dose-dependent manner. Nasal swabs from the vehicle-injected control dogs were positive on day 7, potentially because closely housed dogs shared body fluids, as discussed above. Likewise, the baseline sample mean for the high-dose group was minimally positive.

Stool sample group means were dose dependent at day 7 (fig. S1C). By day 90, only the high-dose group remained positive. Like the nasal swabs, stool group means for the controls were positive on days 7 and 45 but returned to below the limit of detection by day 90. Urine group means on day 90 were positive for the mid– and high–vg/μg dose groups, whereas those from the vehicle-injected and low-dose groups were negative (fig. S1D).

Different AAV serotypes have variable distribution patterns and tissue tropism, with AAV9 demonstrating relative tropism for skeletal muscle and the heart in mice after systemic injection (*30*). In our study, most tissues showed dose-related positivity (>100 vg copies/μg gDNA) at day 90, with considerable overlap and similar concentrations in skeletal muscles and the heart (Fig. 2 and fig. S1, E

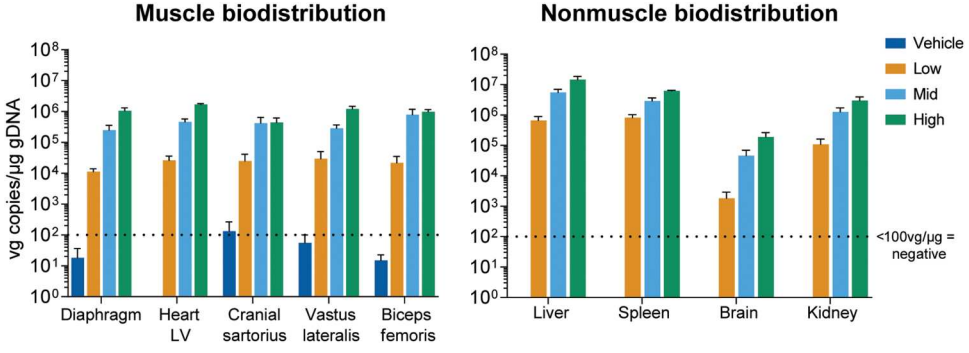

Fig. 2. Biodistribution of vector genomes. Quantitative polymerase chain reaction analysis of vector genome copies per microgram of genomic DNA in muscles (left) and nonmuscle tissues (right) at study day 90. Means and SD for all study participants within a dose group and time point are plotted. LV, left ventricle.

and F). The vg group means in tissues collected from vehicle-injected control dogs remained below the positive cutoff, except for the left cranial sartorius (133 vg/μg gDNA) and thyroid (107 vg/μg gDNA).

Dose-dependent increases in μDys5 expression were observed in AAV-μDys5–treated GRMD dogs

We have previously shown widespread skeletal muscle and, to a lesser extent, cardiac expression of AAV9-transgene constructs after intravenous injection in both wild-type (WT) (*31*) and GRMD (*26*) dogs using nonspecific Rous sarcoma virus and CMV promoters, respectively. In the current study, muscle-specific expression was achieved using the CK8e regulatory cassette derived from enhancer and promoter regions of the muscle creatine kinase gene (*16*).

Quantitation of microdystrophin-positive fibers by immunofluorescence (IF) after AAV-microdystrophin–based therapy in DMD (*32*) and GRMD (*33*) is confounded by the presence of dystrophin-positive "revertant fibers," which presumably result from alternative splicing that reestablishes the mRNA reading frame. To help distinguish revertant and μDys5-positive fibers, we used two dystrophin monoclonal antibodies, one against exon 44 (MANEX44A) (*34*) and one against exons 77 to 79 (DYS2) (fig. S2, A and B). The MANEX44A antibody is selective for spectrin-like repeat R17 of human dystrophin and has cross-species compatibility for canine dystrophin and rAAV9-CK8e-c-μDys5 microdystrophin. DYS2 is reactive to a sequence in the C-terminal region of dystrophin not found in μDys5 microdystrophin.

The average percentage of the cross-sectional area containing skeletal muscle fibers positive for DYS2 staining across all doses, muscles, dogs, and time points ranged from 0 to 1%, in keeping with the absence of full-length dystrophin other than baseline revertant fibers (fig. S2B). Average protein expression for μDys5 via MANEX44A staining at baseline in the vastus lateralis and cranial sartorius muscles ranged from 0 to 0.3%, consistent with the values for DYS2 staining (fig. S2B), confirming that no μDys5 was present before dosing. At the interim time point (about day 45), the biceps femoris exhibited a clear dose response, with group means for μDys5 expression ranging from 0.3% for the vehicle-injected control group to 88.3% for the high-dose group (fig. S3, A and B).

The tissue distribution of μDys5 protein expression was quantified according to the percentage of tissue section area that included positive myofibers or cardiomyocytes. With respect to this end point, a comparable dose response was observed at the terminal (about day 90) time point, with group means ranging from 5.3 to 93% for the low- and high-dose groups (Fig. 3A, fig. S4, and table S2). Area positivity in the low-dose group ranged from 1.3% in the gastrocnemius and vastus lateralis to 20.8% in the semitendinosus (table S2). For the mid-dose group, the average was 61.0%, ranging from a minimum of 30% in the diaphragm to 73.3% in the semitendinosus and vastus lateralis. The average for the high-dose group was 79.2%, with the maximum seen in the semitendinosus and biceps femoris (93%) and minimum in the diaphragm (58.3%). Across all dose groups, the semitendinosus exhibited the highest percentage of cross-sectional area positive for μDys5 expression and the diaphragm exhibited the lowest. All control samples were negative for μDys5 via MANEX44A staining other than baseline skeletal muscle revertant fibers.

For cardiac muscle, the low-dose group had a <1% increase in the average cross-sectional area positive for μDys5 compared with the vehicle-injected controls (figs. S4 and S5). The average overall percentage of cardiac sample positive for μDys5 for the mid-dose group was 9.7%, with a maximum percentage in the left ventricle (LV) (15%) and minimum in the right ventricle (RV) (6%). For the high-dose group, the average overall percentage of cardiac sample area positive for μDys5 expression was 26.7%, with a maximum in the interventricular septum (IVS) (33.3%) and minimum in the RV (18.3%).

To better determine the functionality of μDys5, we assessed four additional proteins in terminal biceps femoris samples—β-sarcoglycan [43-dystrophin-associated glycoprotein (DAG)], developmental myosin heavy chain (MHCd), utrophin, and nNOS. We expected that β-sarcoglycan would be restored by microdystrophin expression and that the reduced drive for muscle turnover in treated dogs would lessen expression of both MHCd and utrophin. In the absence of the nNOS-binding domain, DMD and canine dystrophic muscle is more susceptible to functional ischemia (*35*, *36*). With its inclusion in the μDys5 transgene and restoration of the dystrophin-associated complex in treated dogs, increased nNOS was anticipated.

Expression of these proteins in the day 90 terminal biceps femoris sections generally followed our projections that β-sarcoglycan and nNOS would increase while utrophin and MHCd decreased, each in a dose-responsive manner (Fig. 3A and table S3). A similar pattern was seen in the interim day 45 biopsy samples (table S4).

Protein expression was also determined by Western blot (WB). Densitometry was recorded in single bands at ~427 kDa for dystrophin and ~147 kDa for μDys5. μDys5 protein concentrations at day 90 were below the limit of quantification (BLOQ; <10%) for each dose in the liver and for all muscle samples from the vehicle-injected control and low-dose groups (Fig. 3B, fig. S6, and table S5). Other nontargeted tissues were not tested. Group mean protein expression ranged from 12.6 to 30.5% of normal dystrophin for the mid-dose group and 28.3 to 53.4% in the high-dose group (Fig. 3B). The twofold increase in dose resulted in a 2.8-fold increase in expression in the diaphragm, about a twofold increase in the left ventricle, and a range of 0.9- to 2.8-fold increase in skeletal muscles assessed (table S6).

To further quantify μDys5 protein, we performed mass spectrometry (MS) using protocols modified from previously published methods (*37*, *38*) in which values were given as the percentage of normal dystrophin protein expression. μDys5 protein concentrations were BLOQ (<10%) for all muscle samples from the vehicle-injected controls. One biceps brachii sample was 10% of normal in the low-dose group. Group mean concentrations ranged from 14.6 to 46.7% for the mid-dose group and from 26.6 to 61.3% in the high-dose group (table S7). The twofold increase from 1×10^{14} to 2×10^{14} vg/kg for the mid- and high-dose groups resulted in a 3.2-fold increase in expression in the diaphragm, about a 1.6-fold increase in the LV, and from 1.0- to 3.2-fold in skeletal muscles assessed (table S8). Values for WB and MS strongly correlated (Spearman $r = 0.87$; $R^2 = 0.75$; $P < 0.0001$) (fig. S7).

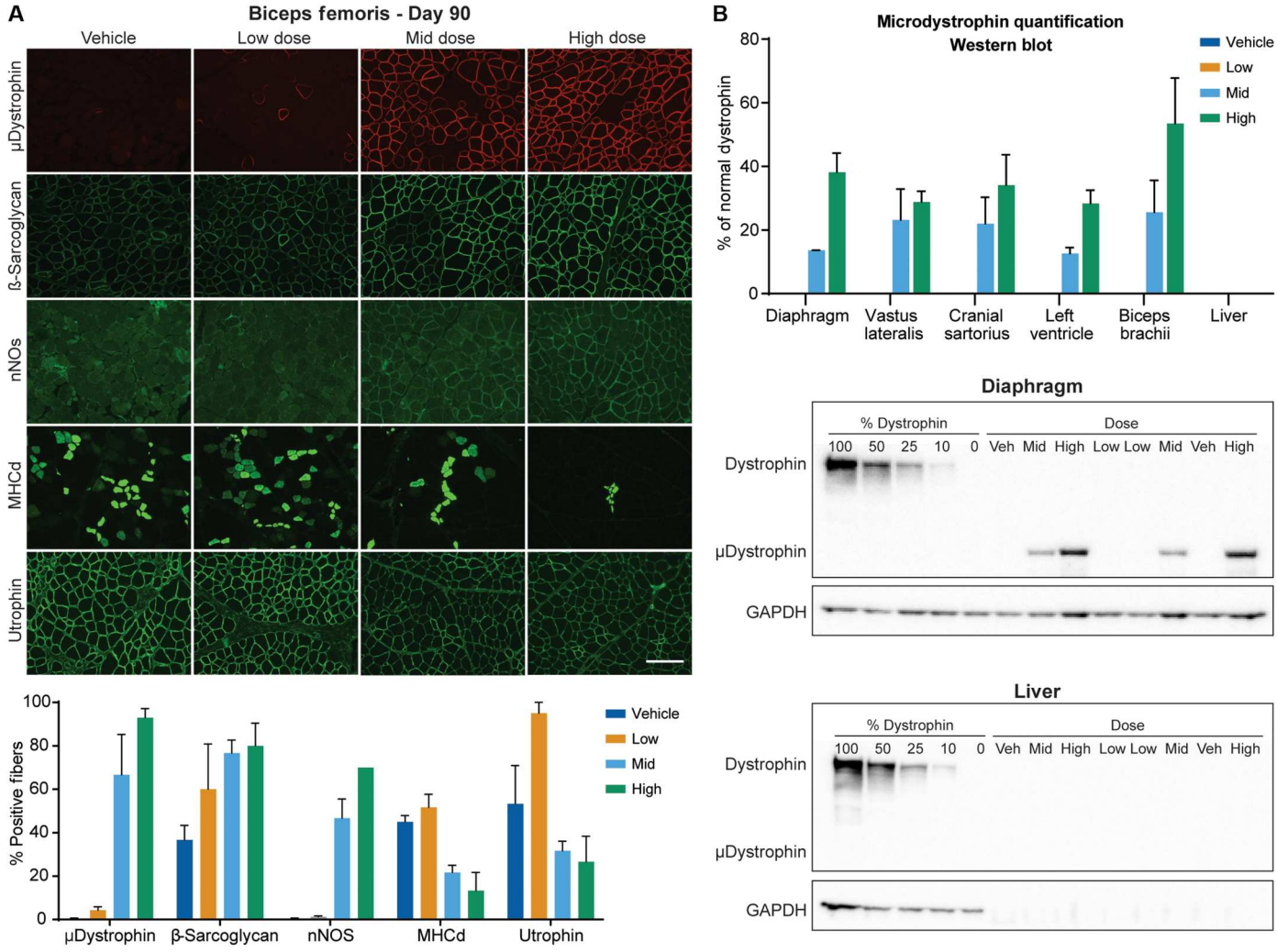

Fig. 3. Protein expression quantified by IF and WB. (**A**) Imaging by IF of biceps femoris muscle sections at day 90 (top) and a histogram depicting group means of the percentage of cross-sectional area containing positive fibers (bottom). Antibody-mediated IF stains include microdystrophin (top row, red), the dystrophin glycoprotein complex members β-sarcoglycan and nNOS (rows 2 and 3; both green), MHCd (row 4, green), and utrophin (row 5; green). Scale bar, 100 µm. (**B**) WB quantification of microdystrophin protein in tissues collected from dogs at necropsy as a percentage of normal dystrophin (top). Each blot (middle: diaphragm; bottom: liver) contains 13 lanes in the following order: Lanes 1 to 5—Dystrophin standard curve composed of 100, 50, 25, 10, and 0% of normal dystrophin; lanes 6 to 13—vehicle, mid, high, low, low, mid, vehicle, high. GAPDH (glyceraldehyde-3-phosphate dehydrogenase) was used to confirm sample loading.

Anti-AAV9 circulating antibodies were absent at baseline, positive at day 7, and largely persisted at day 90

We saw a dose-related increase in anti-AAV9 circulating antibodies in treated GRMD dogs (fig. S8 and table S9). Control, baseline, and day 1 and day 3 samples were negative (<6000 mU/ml, positive cutoff). Antibodies were detected starting at day 7 and increased further on day 16 (fig. S8 and table S9). Most of these differences were not statistically significant when compared across dose groups. Some control values were higher than baseline on day 7 and subsequent measurements but remained below the 6×10^3 threshold for positivity. This minor increase could have occurred because of cohousing, as with the AAV DNA.

Antibodies plateaued beyond day 16, with relatively minor further increases. The high-dose group consistently had a higher trajectory except for a dip at day 61 (fig. S1) when a blood sample was inadvertently not collected, potentially causing an artifactually lower value.

By day 90, all dose groups showed a slight decrease in circulating antibodies. All concentrations remained above baseline, but the difference was only significant between the high-dose and vehicle groups ($P < 0.05$). The average peak for all dose groups was 3.91×10^7 mU/ml, about a 6.5×10^3–fold increase over the positive cutoff. By day 90, this had decreased to an average of about a 4.5×10^3–fold increase, and concentrations did not differ across dose groups.

AAV9-µDys–treated dogs had anti-dystrophin antibodies on WB at day 90 after administration

In addition to AAV-directed humoral immunity, there is the potential for a response to microdystrophin acting as a neoantigen (*3*). Studies in the mdx mouse have suggested that dystrophin-positive

"revertant fibers" may provide tolerance (*27*). However, GRMD dogs treated systemically with an AAV2/8-microdystrophin did demonstrate anti-dystrophin antibodies (*24*). Moreover, mdx mice in which dystrophin was restored through morpholino-induced exon skipping developed antibodies to both full-length and truncated exon-skipped dystrophin isoforms (*39*). To further clarify this issue, we measured immunoglobulin G (IgG) antibodies toward the 427-kDa full-length dystrophin and 147-kDa microdystrophin proteins. Extracts from normal dystrophin-positive, GRMD dystrophin-negative, and AAV9-μDys-treated, microdystrophin-positive GRMD muscle samples were probed using an anti-dystrophin–positive control antibody or sera from animals in vehicle- and AAV9-μDys–treated groups as the primary antibody. IgG antibodies toward both proteins were observed, with the response to microdystrophin being dose dependent (fig. S9).

Dose-related lowering of skeletal muscle histopathologic lesion scores and fibrosis was seen in AAV9-μDys5–treated dogs

Pathologic studies were done to assess potential toxicity and efficacy. No test article-related toxicologic changes were found upon histopathologic assessment of a range of nonmuscle tissues 90 days after dose administration. Microscopic lesions were assessed in skeletal muscles at baseline (day 0), day 45, and terminally at day 90 and the heart at day 90 to show potential efficacy (Fig. 4, A to C).

We biopsied two muscles with distinctive phenotypes, the cranial sartorius (*33*) and vastus lateralis (*40*), at baseline to assess the degree of preexisting disease and treatment effect. On the basis of a semiquantitative grading system of dystrophic pathology (see Supplementary Materials and Methods), histopathologic lesions at baseline ranged from mild/moderate to moderate for the vastus lateralis and from mild to mild/moderate for the cranial sartorius (table S10).

Overall tissue histopathology was generally improved after treatments with mid and high vector doses. At the day 45 interim time point, lesions observed in the biceps femoris were less pronounced in treated dogs, ranging from moderate/severe for vehicle-injected controls to very mild for the high-dose group (fig. S3C and table S10). Lesion scores tracked inversely with microdystrophin IF at day 45 (fig. S3, B and C). A similar dose-related effect was seen in the biceps femoris and other muscles at the terminal (day 90) time point, because mid dose– and high dose–treated dogs had less severe lesions compared with the low-dose and vehicle-injected controls (Fig. 4, A to C).

All samples at baseline and from the interim biopsies and necropsy showed inflammation characteristic of primary dystrophic changes. Inflammation was generally restricted to areas of active myofiber degeneration and regeneration and only extended beyond necrotic regions in tissues scored as "severe." Comparing lesion severity across dose groups, most muscles had moderate/severe lesions in the controls, whereas none of the dogs in the high-dose group had severe scores (Fig. 4C). There was no evidence of inflammation in the rAAV9-CK8e-c-μDys5–treated dogs beyond that seen in vehicle-injected controls. Cell infiltrates typical of inflammatory myopathy were not observed.

Because fibrosis occurs by 6 months in GRMD dogs (*41*), staining for collagen in terminal necropsies at this age could identify a treatment effect. Biceps femoris muscle from dogs in the mid-dose (13.0 ± 2.7) and high-dose (12.4 ± 3.9) dose groups had lower collagen percentages of positive areas on Masson's trichrome stains compared with the control (19.2 ± 5.2) and low-dose (19.1 ± 3.0) groups (Fig. 4D). Although individual dose groups and the controls did not differ, the combined mid-/high-dose groups had significantly lower areas (12.6 ± 2.7) than the combined control/low-dose (19.2 ± 3.4) ($P < 0.01$) dogs.

Calculation of fiber size diameter provides important, albeit indirect, evidence of disease progression and, in turn, response to treatment in both DMD (*42*) and GRMD (*40*). Populations of either smaller or larger myofibers can occur, owing to the combined effects of regeneration and compensatory hypertrophy. We hypothesized that less necrosis in treated dogs would reduce the need for regeneration, resulting in fewer smaller fibers and a higher mean fiber diameter. Although the differences between treated and control dogs were not significant, dogs from the mid-dose (22.5 ± 2.4; $P = 0.68$) and high-dose (25.4 ± 0.39; $P = 0.12$) groups had larger fiber means compared with the control (21.4 ± 2.9) and low-dose (20.6 ± 1.8; $P = 0.77$) groups (Fig. 4E). The high-dose dogs had more fibers in the larger fiber bins. Differences between the combined control/low-dose (21.0 ± 2.4) and mid-/high-dose (24.0 ± 2.2) groups were more pronounced, with a trend toward significance ($P = 0.07$). All LV, RV, and IVS heart samples were designated as normal for all dose groups.

MRI of skeletal muscle did not show evidence of efficacy in AAV9-μDys5–treated dogs

Skeletal muscle magnetic resonance imaging (MRI) has been used as a surrogate biomarker for DMD, showing greater sensitivity than functional tests in natural history studies and clinical trials (*43*). We have also used MRI to define the progression of GRMD (*44*) and response of affected dogs to therapy (*28*). Data from MRI and nuclear magnetic spectroscopy collected from two GRMD dogs treated with an AAV-microdystrophin construct showed changes reflecting a reduction in lesion severity (*24*). For the studies reported here, methods developed by our group at the University of North Carolina-Chapel Hill (UNC-CH) were used at Texas A&M using a similar Siemen's 3T MRI unit. Biomarkers found to distinguish lesions of GRMD dogs from WT canine muscle at UNC-CH (*44*) were assessed at baseline and day 90. Upon analyzing changes in these biomarkers between days 0 and 90, there were few differences across the dose groups and no overall pattern suggesting efficacy (table S11).

AAV9-μDys5–treated dogs exhibited dose-related percent changes in muscle torque

Studies in large animal models often are underpowered because of practical considerations relating to cost and availability. In comparing the percent gain in μDys5 cross-sectional IF staining among dog groups, we noted that the average percentage positive for μDys5 expression for the mid-dose (1×10^{14} vg/kg) dogs was 21.5-fold higher than the low-dose (1×10^{13} vg/kg) dogs, whereas the increase was limited to 1.3-fold between the mid and high (2×10^{14} vg/kg) doses. Given this dose effect, to increase the study's power, we subsequently compared limb and respiratory functional data from the combined control and low-dose groups to those of the combined mid- and high-dose dogs.

We have sought to develop muscle function outcome methods in GRMD dogs that parallel those used in DMD and mdx mice. Tests to measure extension and flexion tibiotarsal joint (TTJ) torque (*45*),

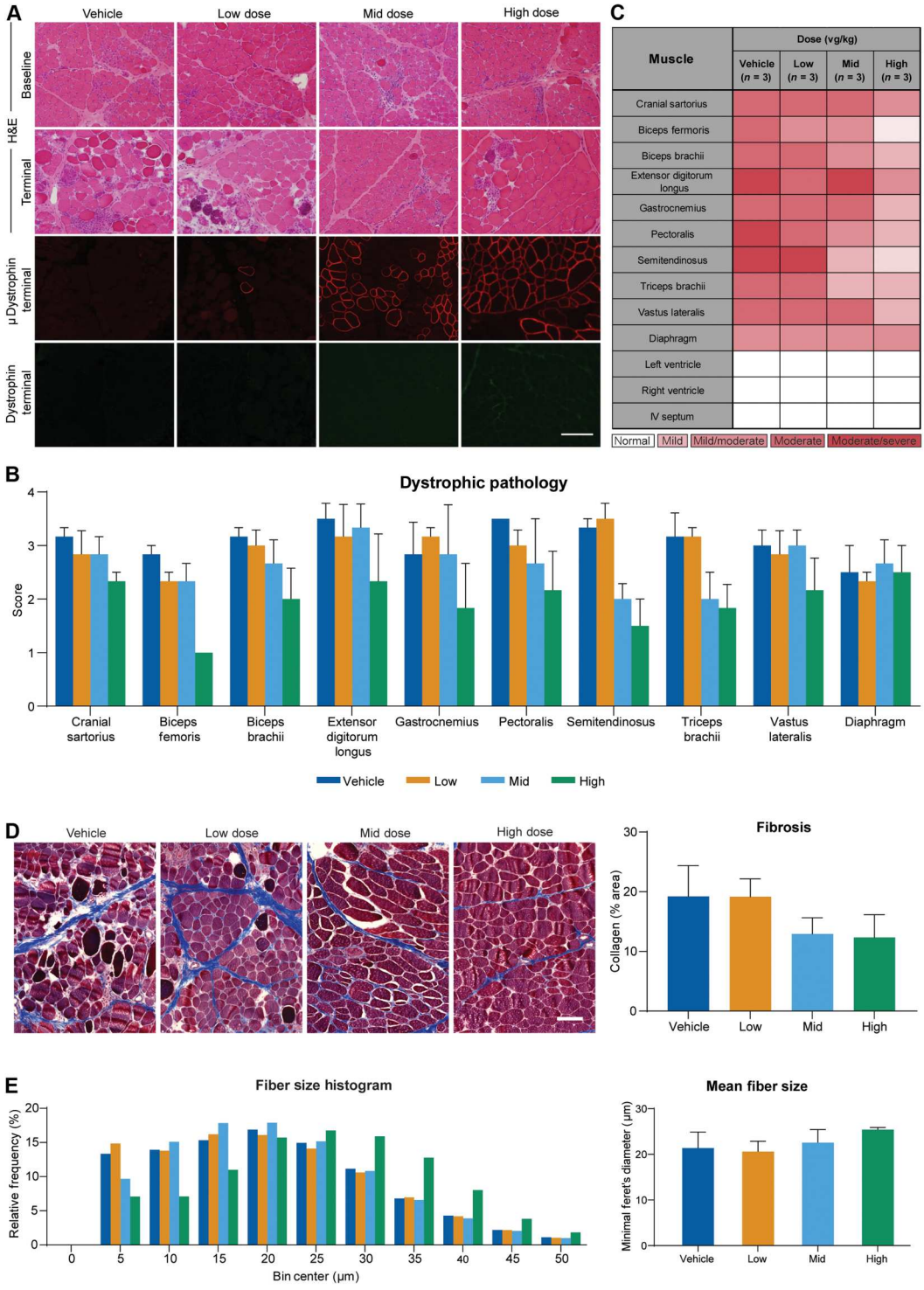

Fig. 4. AAV9-µDys5–treated dogs demonstrate reduced histopathologic lesions and fibrosis. (**A**) Images of cranial sartorius muscle at baseline and day 90 from GRMD dog with hematoxylin and eosin staining (top two panels). IF of microdystrophin (red) and dystrophin (green) at day 90 (bottom two panels). (**B**) Average lesion scores varied across skeletal muscles but were generally lower in the mid- and high-dose groups. (**C**) A heatmap demonstrating lesion severity in skeletal muscle and cardiac samples from all dogs obtained at day 90. (**D**) Representative images from each dose group of muscle collected at necropsy and stained with Masson's trichrome (left), together with a histogram of mean collagen per group quantified as a percent of area (right). (**E**) Data presented as a histogram of relative frequency of fiber size using 5-µm bins up to a maximum of 50 µm and mean fiber size for each dose group (left). Fiber size evaluation of biceps femoris muscles collected at necropsy using minimal Feret's diameter measurements (right). Scale bar, 100 µm (A and D).

6-minute–walk test (6MWT) (*46*), extension contraction decrement (ECD) (*47*), and joint angles (*29*) have now been used in several GRMD preclinical trials (*11*, *28*, *48*). Dogs were assessed using these tests at baseline and 45 and 90 days after treatment.

Strength must be considered in the context of potential treatment effects on body size. Body mass (in kilograms) is lower in GRMD versus WT dogs at 3, 4.5, 6, and 12 months (*45*). Proportionally greater increases could suggest treatment benefit. In tests of TTJ torque, neither baseline nor absolute/percent change values at day 90 differed across individual or combined groups (Table 1). Absolute and body mass–corrected torque values in Newton-meters (Nms; force in Newtons × the lever arm length in meters) were determined. Percent change was calculated from day 0 to interim and results at days 45 and 90. Extension torque has best defined a treatment effect in other GRMD studies (*28*, *48*) and was viewed as the primary outcome parameter.

Torque values did not differ across the four treatment groups at baseline (day 0) ($P > 0.05$) (Table 1). Dose-related treatment effects were seen at day 45 and became more pronounced at day 90. Differences were best reflected by percent change from baseline to day 90. A dose-effect across individual dose groups became more marked when the combined data were compared (Fig. 5A) and could also be seen when percent change in absolute extension (Fig. 5B) and flexion (Fig. 5C) torque from day 0 to days 45 and 90 was plotted.

As an example of the overall pattern, although the percent change for absolute tetanic extension torque from days 0 to 45 only trended toward being significantly higher in the mid-dose group (237 ± 96) versus controls (101 ± 87) ($P = 0.10$), the difference reached significance at day 90 (374 ± 59 versus 161 ± 126; $P < 0.01$) (Table 1). Further reflecting the dose effect, differences for the high-dose versus control groups were significant at both time points ($P < 0.05$ at day 45 and $P < 0.001$ at day 90). Absolute extension torque percent change values were more pronounced when the combined data for the mid-/high-dose and control/low-dose groups were compared (465 ± 107 versus 162 ± 83; $P < 0.001$) (Fig. 5B). Body mass–corrected values showed less pronounced differences, with percent change from days 0 to 90 for extension torque only trending toward being significantly higher in the combined mid-/high-dose (120 ± 43) versus control/low-dose (31 ± 68) ($P = 0.06$) dogs.

The flexion torque and percent change values generally tracked with those for extension, but changes tended to be more pronounced, showing evidence of earlier treatment effects (Fig. 5B and Table 1). For example, even with the mid-dose group alone, the percent change for absolute tetanic flexion from days 0 to 45 (211 ± 71) was significantly higher than for controls (54.9 ± 74) ($P < 0.05$). The difference was even more pronounced at day 90 (285 ± 65 versus 118 ± 41; $P < 0.01$). Percent change for body mass–corrected flexion at day 90 was also significantly higher for the combined mid-/high-dose (80.8 ± 42) versus control/low-dose (17.4 ± 27) dogs ($P < 0.05$).

On comparisons of 6MWT results across individual groups, the high dose–treated dogs walked further absolute distances (in meters) than controls at day 90 (348 ± 163 versus 170 ± 147), with an associated higher percent change from baseline (56.5 ± 79 versus 13.2 ± 95.36) (Table 1). Comparable differences in absolute distances walked (290 ± 124) and percent change (107 ± 105) were seen in the combined high-/mid-dose versus control/low-dose (176 ± 102, 10.2 ± 78) dogs. The mid-dose dogs had decidedly lower baseline values, which could have artificially led to a greater apparent treatment effect. Regardless, with the small group sizes and large SD values, none of these differences reached significance ($P = 0.26$ and 0.27 for the combined groups). Analogous differences were seen for height-adjusted distance walked.

Values for ECD from 0 to 30 stimulations in some individual dogs suggested a potential treatment effect at day 90 but did not differ when compared across groups and over particular time periods (Table 1). For example, the ECD of the high dose–treated dogs at day 90 was lower than in the controls, 37.7 ± 16 versus 51.0 ± 17, but the *P* value was only 0.72. Moreover, the 1 to 30 stimulation ECD values for the combined control/low-dose (53.3 ± 12) and mid-/high-dose (51.3 ± 20) dogs were essentially identical ($P = 0.96$). Occasional outlier values made it impossible to interpret percent change for the different time periods across the groups. There were few differences between joint angles in treated and control dogs. The overall pattern of changes did not suggest a treatment effect (table S12).

Respiratory function was less impaired in AAV9-μDys5–treated dogs

Cardiopulmonary disease is a major cause of morbidity and mortality in patients with DMD (*49*). We have previously shown objective evidence of pulmonary dysfunction by assessing respiratory inductance plethysmography (RIP) in adult GRMD versus phenotypically normal carrier dogs (*50*). Dystrophic dogs had markedly higher tidal breathing peak expiratory flows (PEF), with an associated increase in peak expiratory flow–to–peak inspiratory flow (PEF:PIF) ratios. Anticipating, because we ultimately showed (*51*) that similar changes would be seen in younger GRMD dogs, we compared the RIP PEF:PIF ratio across the treatment groups at day 90 and for percent change from days 0 to 90 (Fig. 6, A to C, and Table 1). The major differences were seen at day 90, with the PEF:PIF ratios for the mid dose (1.55 ± 0.31)– and high dose (1.63 ± 0.23)–treated dogs being lower than that of the control group (2.38 ± 0.11) ($P < 0.01$ for both). The PEF:PIF ratios for low-dose/control dogs increased over time, whereas those for the mid-/high-dose dogs were relatively stable (Fig. 6B). Differences were more pronounced when data from the combined mid-/high-dose (1.59 ± 0.25) and control/low-dose (2.29 ± 0.37) groups were compared ($P < 0.001$) (Fig. 6C, left). The percent change in PEF:PIF ratios for individual and especially combined groups also showed a treatment effect (Fig. 6C, right, and Table 1). Values for the combined mid-/high-dose dogs were relatively stable from baseline to day 90 (3.84 ± 14; $P = 0.74$) compared with a marked increase (48.1 ± 19; $P < 0.001$) typical of disease progression in the control/low-dose dogs.

Cardiac indices did not differ between AAV9-μDys5–treated and control dogs

We and others have conducted systematic studies of cardiac function in GRMD dogs. The findings have generally pointed toward a delayed onset of cardiac dysfunction, in keeping with DMD cardiomyopathy (*52*). Accordingly, we did not expect a treatment effect over the 3- to 6-month age period and were primarily motivated to assess safety.

All electrocardiograms at baseline and study days 45 and 90 were qualitatively and quantitatively within normal limits (table S13). No

Table 1. Skeletal muscle limb and respiratory function tests (mean ± SD) Significantly different versus control or combined control/low dose; *$P < 0.05$, **$P < 0.01$, ***$P < 0.001$; #Only one dog had measurements at both days 0 and 45; ECD, eccentric contraction decrement.

Group–study day	Body mass (kg)	Absolute tetanic torque (Nm)		Mass-corrected tetanic torque (Nm/kg}		ECD (1–30) (%)	6MWT		PEF:PIF ratio
		Extension	Flexion	Extension	Flexion		Absolute distance (m)	Height adjusted (m/cm)	
Low dose									
0	6.30 ± 2.3	1.00 ± 0.38	0.36 ± 0.19	0.21 ± 0.04	0.07 ± 0.01	57.7 ± 17	204 ± 84	6.59 ± 3.4	1.43 ± 0.18
45	8.23 ± 2.4	2.57 ± 2.1	0.69 ± 0.18	0.29 ± 0.18	0.08 ± 0.01	55.7 ± 8.7	213 ± 25	5.70 ± 0.98	1.62 ± 0.02
% Change (0–45)	33.9 ± 24	136 ± 107	120 ± 86	40.1 ± 85	20.8 ± 26	−0.18 ± 18	−7.86 ± 21	−27.0 ± 15	17.5 ± 22
90	9.37 ± 1.3	2.71 ± 1.4	0.86 ± 0.22	0.27 ± 0.13	0.09 ± 0.01	55.7 ± 7.4	181 ± 65	4.19 ± 1.3	2.20 ± 0.55
% Change (0–90)	58.0 ± 38	162 ± 40	173 ± 100	29.3 ± 64	24.2 ± 9.6	2.55 ± 32	7.23 ± 77	−16.7 ± 67	53.3 ± 23
Mid dose									
0	6.17 ± 0.64	0.92 ± 0.15	0.30 ± 0.06	0.20 ± 0.03	0.07 ± 0.02	44.0 ± 19	98.9 ± 29	3.05 ± 0.86	1.48 ± 0.09
45	9.63 ± 0.68	3.01 ± 0.43	0.90 ± 0.12	0.31 ± 0.03	0.09 ± 0.10	71.7 ± 8.1	264 ± 110	6.45 ± 2.4	1.50 ± 0.42
% Change (0–45)	57.9 ± 25	237 ± 96	211 ± 71*	57.0 ± 28	80.2 ± 19	84.6 ± 77	229 ± 254	150 ± 179	2.87 ± 23
90	10.7 ± 1.1	4.31 ± 0.31	1.12 ± 0.08	0.38 ± 0.05	0.10 ± 0.02	65.0 ± 16	233 ± 41	5.28 ± 0.86	1.55 ± 0.31**
% Change (0–90)	75.1 ± 33	374 ± 59**	285 ± 65**	95.0 ± 43	110 ± 24	67.1 ± 71	158 ± 117	87.1 ± 73	3.77 ± 16**
High dose									
0	5.90 ± 0.30	0.72 ± 0.13	0.28 ± 0.07	0.17 ± 0.01	0.06 ± 0.01	36.0 ± 22	231 ± 86	7.44 ± 2.8	1.56 ± 0.05
45	9.40 ± 1.5	2.93 ± 1.1	1.09 ± 0.15*	0.29 ± 0.07	0.11 ± 0.03	55.0 ± 6.6	298 ± 72	7.44 ± 1.5	1.55 ± 0.36
% Change (0–45)	58.9 ± 25	297 ± 80*	294 ± 77**	70.1 ± 33	80.2 ± 46	119 ± 166	62.2 ± 9.4	25.7 ± 2.7	18.47#
90	11.7 ± 1.2	4.74 ± 0.79*	1.51 ± 0.39**	0.42 ± 0.05	0.13 ± 0.03*	37.7 ± 16	348 ± 163	7.85 ± 3.6	1.63 ± 0.23**
% Change (0–90)	97.5 ± 14	557 ± 15***	435 ± 54***	145 ± 30	110 ± 37*	24.9 ± 51	56.5 ± 79	9.12 ± 53	3.95 ± 18**
Controls									
0	6.50 ± 0.50	1.13 ± 0.28	0.42 ± 0.05	0.21 ± 0.06	0.08 ± 0.01	52.0 ± 32	165 ± 37	5.00 ± 1.1	1.70 ± 0.05
45	9.53 ± 1.4	2.11 ± 0.37	0.66 ± 0.32	0.24 ± 0.04	0.08 ± 0.04	56.7 ± 25	110(n = 1)	2.61 (n = 1)	1.81 ± 0.12
% Change (0–45)	18.8 ± 5.8	101 ± 87	54.9 ± 74	23.6 ± 55	5.29 ± 57	31.3 ± 86	−43.7 (n = 1)	−57.1 (n = 1)	3.42#
90	11.4 ± 2.2	2.73 ± 0.58	0.91 ± 0.14	0.25 ± 0.09	0.08 ± 0.03	51.0 ± 17	170 ± 147	5.84 ± 1.1	2.38 ± 0.11
% Change (0–90)	74.2 ± 24	161 ± 126	118 ± 41	33.2 ± 87	10.6 ± 40	25.9 ± 77	13.2 ± 95	30.9 ± 0.56	40.4 ± 13
Combined control/low dose									
0	6.40 ± 0.60	1.07 ± 0.31	0.39 ± 0.13	0.21 ± 0.05	0.07 ± 0.01	54.8 ± 23	184 ± 62	5.80 ± 2.4	1.54 ± 0.20
45	8.88 ± 1.9	2.34 ± 1.4		0.27 ± 0.12		56.2 ± 17	178 ± 62	4.67 ± 1.9	1.72 ± 0.13

continued on next page

Group–study day	Body mass (kg)	Absolute tetanic torque (Nm)		Mass-corrected tetanic torque (Nm/kg}		ECD (1–30) (%)	6MWT		PEF:PIF ratio
		Extension	Flexion	Extension	Flexion		Absolute distance (m)	Height adjusted (m/cm)	
			0.68 ± 0.23		0.08 ± 0.02				
% Change (0–45)	40.1 ± 19	118 ± 89	87.4 ± 80	31.8 ± 65	13.1 ± 40	15.6 ± 58	−19.8025	−37.1 ± 20	12.8 ± 18
90	10.4 ± 2.0	2.72 ± 0.97	0.89 ± 0.17	0.26 ± 0.10	0.09 ± 0.02	53.3 ± 12	176 ± 102	4.85 ± 1.4	2.29 ± 0.37
% Change (0–90)	66.1 ± 30	162 ± 83	145 ± 75	31.2 ± 68	17.4 ± 27	14.2 ± 54	10.2 ± 78	2.33 ± 54	48.1 ± 19
Combined mid/high dose									
0	6.03 ± 0.47	0.82 ± 0.16	0.29 ± 0.06	0.19 ± 0.02	0.07 ± 0.01	40.0 ± 19	165 ± 93	5.24 ± 3.0	1.51 ± 0.08
45	9.52 ± 1.1	2.97 ± 0.75	1.00 ± 0.16*	0.30 ± 0.05	0.10 ± 0.02	63.3 ± 11	281 ± 79	6.94 ± 1.7	1.52 ± 0.32
% Change (0–45)	58.4 ± 21	267 ± 86*	252 ± 81**	63.6 ± 28	59.0 ± 39	102 ± 117	146 ± 176	87.7 ± 126	8.07 ± 18
90	11.2 ± 1.2	4.52 ± 0.58**	1.32 ± 0.33**	0.40 ± 0.05*	0.12 ± 0.03*	51.3 ± 20	290 ± 124	6.57 ± 2.8	1.59 ± 0.25***
% Change (0–90)	86.3 ± 26	465 ± 107***	360 ± 98***	120 ± 43	80.8 ± 42*	46.0 ± 60	107 ± 105	48.1 ± 71	3.84 ± 14***

test article–related abnormalities in rhythm, waveform morphology, heart rate, RR interval, PR interval, QRS duration, QT interval, or QTc interval were observed at any dose based on comparison of pre- and postdose group and control values.

Similarly, baseline echocardiography and cardiac MRI were within normal limits (table S14). Values after dosing did not differ between treated and control dogs. Thus, from a safety perspective, AAV9-μDys5 treatment was not detrimental to cardiac function.

Serum muscle enzyme values trended lower in AAV9-μDys5–treated dogs

Hematologic and serum chemistry parameters were assayed to detect evidence of both potential toxicity and efficacy. Hematological changes typical of a stress leukogram (neutrophila with no left shift, lymphopenia, and eosinopenia) were seen in most dogs during prednisone dosing and generally resolved after conclusion of prednisone. No hematologic or chemical changes suggestive of organ injury were seen.

In DMD, certain serum enzymes, including creatine kinase (CK) as well as the transaminases alanine aminotransferase (ALT) and aspartate aminotransferase (AST) (*53*), are elevated. These enzymes are also increased to a lesser degree in BMD patients with in-frame deletions (*54*) and so would not be expected to fully normalize after treatment with AAV-microdystrophin. This is consistent with previous data showing that serum CK was reduced but remained elevated in mdx mice treated with μDys5 (*55*).

In keeping with published findings (*56*), most GRMD dogs had high CK, ALT, and AST values on day −8 before beginning the 5-week course of prednisone (fig. S10 and tables S15 to S17). These baseline values did not differ across dose groups. Regarding values after treatment, consideration should be given to a previous study showing that prednisone can lower CK in GRMD (*57*). With that said, by day 7 (week 1), there was a trend toward lower CK values in the mid dose– and high dose–treated dogs (table S15). This was more pronounced on day 16 (week 3) and persisted through day ~90 (week 13). Demonstration of the dose effect was accentuated by combining CK data from the control/low-dose and mid-/high-dose dogs (fig. S10). Values for serum ALT and AST (tables 16 and 17) generally paralleled CK. There was a considerable overlap of values, but a trend for a dose effect could be seen, with higher group means in the control and low-dose dogs. Overall, none of the serum enzyme differences reached significance.

DISCUSSION

The mdx mouse model of DMD is mildly affected and often underestimates immunologic side effects (*11*, *58*). Outbred dogs more reliably show the immune response to genetic and cell-based therapies (*59*, *60*). An apparent immunologic reaction in dystrophic dogs treated intramuscularly with AAV-microdystrophin (*12*, *13*) was attributed, in part, to interspecies (human versus canine) differences in dystrophin epitopes (*27*) and use of a CMV promoter with resulting dystrophin expression in nonmuscle tissues (*16*). Both of these potential sources of immunity were eliminated in the current study. GRMD dogs treated systemically with AAV9-canine-μDys5 under control of a muscle-specific promoter showed dose-dependent increases in tissue vector genome copy numbers; μDys5 protein in multiple appendicular muscles, the diaphragm, and

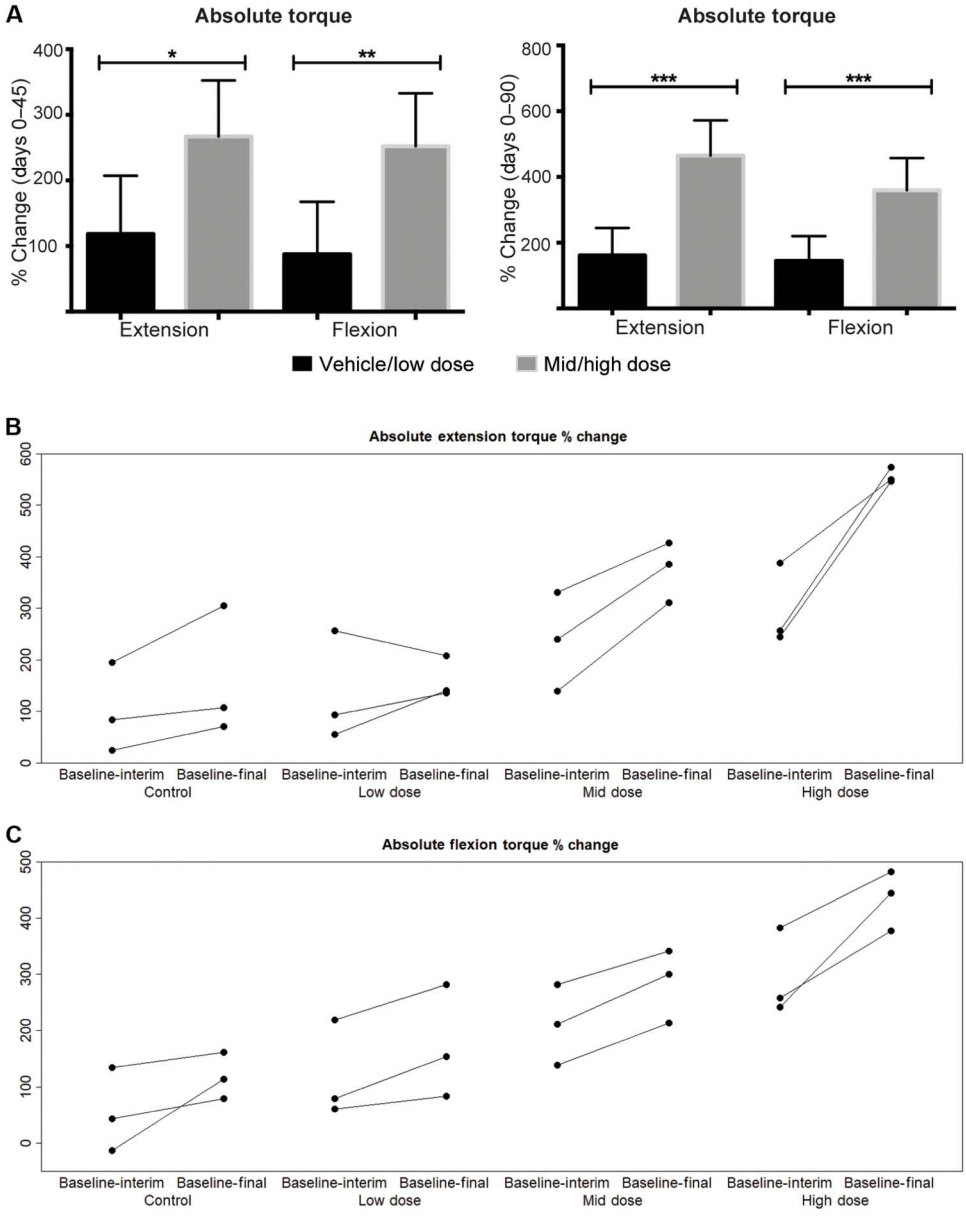

Fig. 5. Absolute tibiotarsal joint extension and flexion torque percent change for combined dose groups from baseline to days 45 (interim) and 90 (final). (**A**) Dose-related increases in the percent change for both absolute extension and flexion torque from baseline to day 45 (left) and to day 90 (right). Means and SD for all study subjects within a dose group and time point are plotted. (**B** and **C**) Percent changes for extension (B) and flexion (C) torque plotted for individual dogs show evidence of a dose effect. Each dose group, $n = 3$; combined dose groups, $n = 6$. Combined control and low-dose versus mid- and high-dose groups were compared using the Mann-Whitney-Wilcoxon test. *$P < 0.05$; **$P < 0.01$; ***$P < 0.001$.

heart; limb and respiratory muscle functional improvement; and a reduction in histopathologic lesions without severe adverse side effects. These results tend to substantiate a role for dystrophin interspecies differences and nonmuscle expression as sources of immunity in microdystrophin therapy. However, direct comparisons in which separate groups of GRMD dogs were treated with human transgene and a nonspecific promoter would be required to confirm this observation.

Speaking further to the potential for an immune response, T cells reacted to microdystrophins on an ELISPOT assay in patients with DMD (*9*, *61*). No positive T cell responses were observed in the limited number of ELISPOTs done in GRMD dogs of our study. Moreover, there was no inflammatory response beyond that typically seen in dystrophic muscle. Tied to the potential for an immune response, questions have been raised about whether sustained dystrophin expression could be achieved with a single treatment (*4*). Dystrophic dogs treated systemically with an AAV2/8-microdystrophin construct showed persistent dose-dependent dystrophin expression for at least 14 months, even without immunosuppression (*24*). Clinical stabilization and reduction of histopathologic changes were evident for as long as 24 months. These findings largely paralleled the therapeutic benefit seen in GRMD dogs reported here.

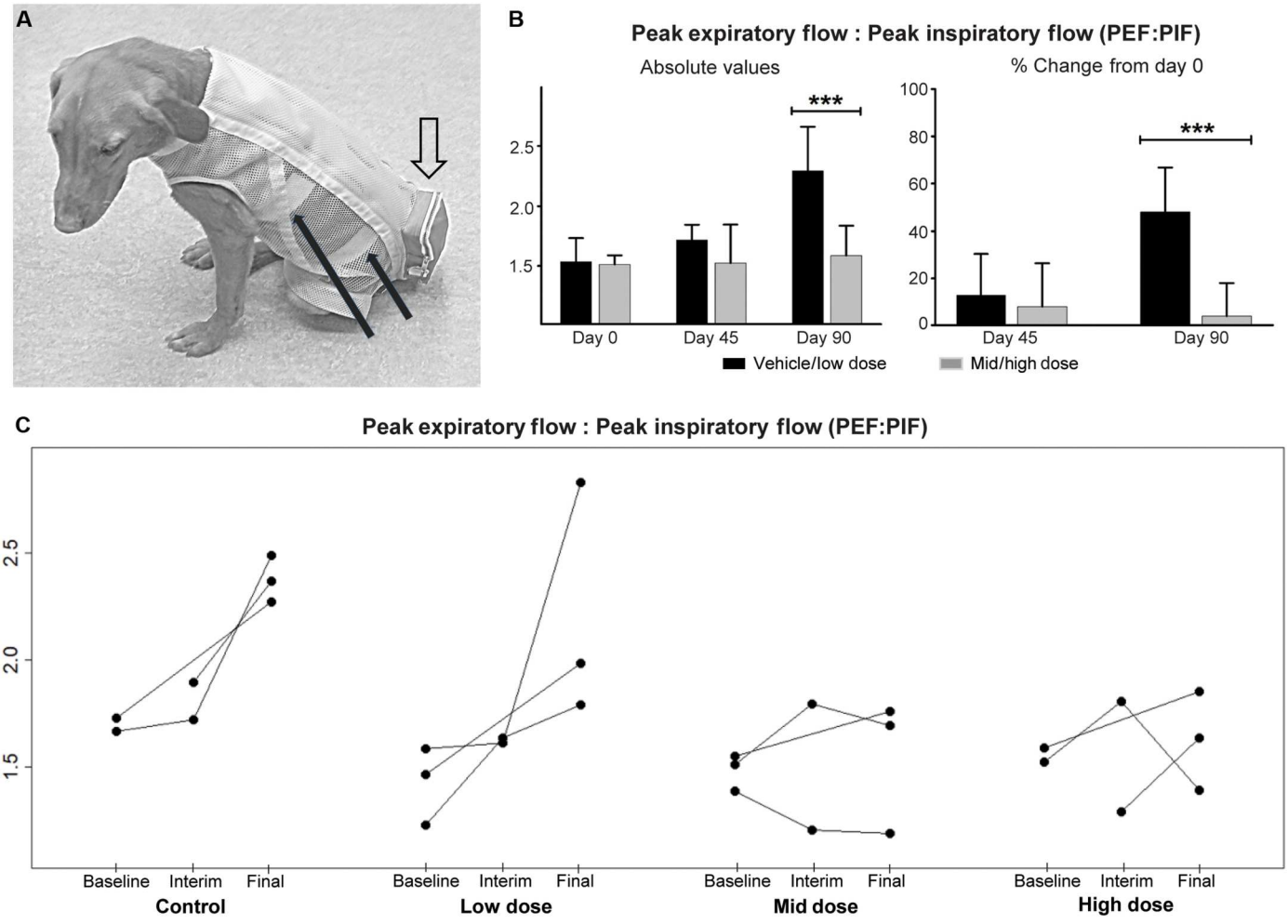

Fig. 6. PEF:PIF ratios from baseline to end of study. (**A**) Adult GRMD dog showing the instrumentation for respiratory inductance plethysmography (RIP). The solid black arrows point to the elastic inductance bands that circle the chest and the abdomen. The bands are looped through an inner Lycra undershirt. Leads from the bands pass through the loose, outer mesh shirt and directly into the telemetry unit within the outer pouch (open arrow). (**B**) Graphs showing the absolute (left) PEF:PIF ratios at day 90 and the percent change from day 0 to days 45 and 90 (right). Each dose group, $n = 3$; combined dose groups, $n = 6$. Combined control and low-dose versus mid- and high-dose groups were compared using the Mann-Whitney-Wilcoxon test. ***$P < 0.001$. (**C**) RIP PEF:PIF ratios for individual dogs show a dose effect, with a disease-associated increase in the control/low-dose dogs compared with relative stability of values for the mid-/high-dose groups.

Our study is the first to assess a microdystrophin systematically tested in mdx mice and then dystrophic dogs in DMD clinical trials.

Beyond concerns about immunity and loss of transgene transduction over time, it has not been clear that <4.7-kb microdystrophins carried by AAV vectors will hold up to rigorous demands placed on muscles by larger animals. Extending mdx studies to dystrophic dogs, Duan and colleagues demonstrated relative phenotypic rescue, including a reduction of ECD and histopathologic changes, after localized AAV-microdystrophin injection in the small extensor carpi ulnaris (ECU) muscle (*15*). A follow-up study in which this same construct was delivered systemically to immunosuppressed GRMD dogs showed widespread dystrophin expression and reduced histopathologic lesions (*23*). However, the ECU had minimal dystrophin expression and no improvement in histopathologic changes or function. The results of our current study are promising because TTJ extension torque, which we have used as the primary outcome parameter in other preclinical trials (*28*, *48*), improved in treated versus control dogs. Still greater improvement was seen for TTJ flexion, with changes noted even in the mid-dose group at the day 45 interim time point. This increase in flexion torque contrasts with a paradoxical decrease seen with both prednisone (*48*, *57*) and a Nemo-binding domain (NBD) peptide (*28*) treatment, probably reflecting the obvious mechanistic differences. Prednisone and NBD peptide reduce inflammation and enhance muscle regeneration, whereas microdystrophin should stabilize the myofiber membrane and decrease eccentric contraction injury. In this study, ECD did not differ between the treated and control dogs, indicating incomplete myofiber protection. Similarly, CK trended lower in treated dogs but remained elevated. Both of these findings would be expected, given that microdystrophin should ameliorate but not cure DMD, enabling a transition to a Becker phenotype (*5*).

With more aggressive respiratory support, cardiomyopathy has supplanted pulmonary complications as the major cause of death in

DMD (*62*). Thus, with any treatment, it is important to target the heart. The AAV9 vector was chosen partly because of its high expression in both cardiac and skeletal muscle (*63*). Similar dual tissue tropism is seen with expression cassettes developed in the Hauschka laboratory (*16*). Supporting the choice of AAV9 under control of a muscle-specific promoter, dose-related increases in μDys5 expression were observed in all sections of the heart assessed. Although the late onset of cardiomyopathy across DMD, the mdx mouse, and GRMD (*52*) precluded demonstrating therapeutic efficacy, the absence of deleterious cardiac effects supported a positive safety profile. More encouragingly, treated dogs showed dose-related improved respiratory function, evidenced by relative stabilization of the PEF:PIF ratio.

There are currently four ongoing DMD AAV-microdystrophin clinical programs (*4*, *5*, *64*), including Solid Biosciences' SGT-001 (https://clinicaltrials.gov/ct2/show/NCT03368742), the human codon-optimized variant of the construct used in this GRMD study. Each is unique to itself, with different inclusion criteria, constructs, doses, and outcome parameters. Data are incomplete, and many methods of analysis are proprietary, making it difficult and premature to compare results across programs. Although no unexpected immune histopathologic or clinical side effects were observed in GRMD dogs treated with SGT-001 reported here, serious adverse events (SAEs) linked to complement activation, including systemic inflammatory response syndrome and thrombocytopenia, have been noted in the ongoing DMD clinical trial (*65*). SAEs have also been documented in the Sarepta, Pfizer, and Genethon microdystrophin gene therapy trials and in patients receiving AAV genetic constructs for other neuromuscular diseases (*66*–*68*).

Several factors could account for the immune response in the DMD trials. Much attention has focused on the established role of AAV in activating complement during the innate immune response (*69*). Given the absence of severe side effects and immunologic abnormalities throughout our study, we did not assess complement or use aggressive immunosuppression regimens. Protein transcribed by the R16/17 spectrin-like repeats of the SGT-001 nNOS binding domain might be a source of immunity. In this context, a recent collaboration among the four programs using AAV-microdystrophin constructs specifically studied the potential role the transgene played in five DMD patients with SAEs. All had genomic deletions involving N-terminal epitopes, with ELISPOTs reactive to the corresponding N-terminal peptide pool (*70*). None of those who received SGT-001 had reactions to the transgene protein.

This study had several limitations. Because of practical issues related to cost and availability, canine studies must always be focused. We were not motivated to repeat studies already done by the Chamberlain laboratory in mice to establish benefits provided by the nNOS binding domain. Similarly, no comparisons were made between human versus canine transgenes or specific versus nonspecific promoters that might have shed light on the immune response. Even when canine studies are focused, they are often marginally powered to detect differences with all outcomes that are assessed. The power of our study was increased by comparing results from the combined control/low- dose and mid-/high-dose groups, but numbers were still relatively low. In addition, despite analyzing combined data, some values showed a wide SD, reflecting variation from dog to dog of μDys5 expression and associated functional and pathologic treatment effect. This likely contributed to the failure of these tests to demonstrate efficacy. Outcomes that are reproducible, with relatively low SDs, are more likely to yield meaningful results. We have generally used TTJ torque as our primary outcome and have had considerably less experience and success using 6MWT, ECD, joint angles, and MRI. Regarding MRI, the Siemens 3T unit and analysis methods were like those used in earlier natural history and treatment studies at UNC-CH (*28*, *44*). Still, minor differences in MRI protocols and analysis methods probably played a role in our inability to distinguish differences at the current sample size. Regardless of these limitations, the results from this blinded, placebo-controlled study in GRMD dogs highlight the promise of AAV-microdystrophin for the treatment of DMD and the utility of large animal models to evaluate alternative therapeutic approaches.

MATERIALS AND METHODS

Study design

This study explored the clinical translatability of an AAV9–microdystrophin construct in the GRMD model of DMD. Dogs (12 total; four groups of three each) received one of three doses (1×10^{13}, 1×10^{14}, and 2×10^{14} vg/kg) of rAAV9-CK8e-c-μDys5 or vehicle intravenously at 3 months of age and were then monitored for 90 days after dosing using a comprehensive set of analyses that included biodistribution, μDys5 protein expression, limb muscle torque, histopathology, clinical pathology, immune response, MRI, and respiratory and cardiac function.

On the basis of power analysis (*45*), we have typically used TTJ extension torque as our primary outcome parameter in GRMD preclinical studies (*28*, *48*). Original natural history studies anticipated that a single measurement at the end of treatment would be compared with a control value. Our preclinical trials have generally assessed five or six dogs in the treatment arm, comparing them with a similar number of untreated dogs (*48*) or natural history controls (*28*).

The original study design called for a two-phased study, with an initial cohort of 12 dogs divided among the three doses and a control group ($n = 3$ for each), as reported here. On the basis of the outcome of these studies, we anticipated that a second cohort of nine GRMD dogs would be assessed, with three each added to the two dose groups having the most promising results and a set of controls ($n = 6$ each). However, after a treatment effect was seen with the 12 dogs of the first cohort, the second phase was canceled.

The 12 dogs were randomly assigned to one of the four groups as they were produced in the GRMD colony at Texas A&M University over an 18-month period (see the "Animals" section below). Study personnel were blinded from dose formulations and animal group assignments throughout the study, including at dose administration and collection of outcome data. Vehicle control dose formulations were identical in visual appearance and viscosity to AAV test article and labeled similarly to all other formulations. The vehicle used for the control group was equivalent to the formulation buffer used for test article manufacturing and was also used to normalize dose formulation volumes for all other groups.

Functional measures were repeated over the 3-month course of the study. Laboratory assessments included an average minimum of two to three technical replicates per assay.

Animals

Dogs were used and cared for according to principles outlined in the National Research Council *Guide for the Care and Use of Laboratory Animals*. Studies were approved by the Texas A&M University (TAMU) Institutional Animal Care and Use Committee (IACUC) through two protocols: TAMU IACUC 2014-0117, Advanced Gene Therapy for Treatment of Cardiomyopathy and Respiratory Insufficiency in Duchenne Muscular Dystrophy, and TAMU IACUC 2017-0248, Gene Therapy for Duchenne Muscular Dystrophy. Although phenotypic data have not distinguished a difference between male hemizygous and female homozygous GRMD dogs (*71*), an effort was made to balance males and females among the different dose and control groups. This was achieved with the inclusion of six males and six females.

Statistical analysis

Means and SDs for body mass, skeletal muscle limb functional, and respiratory data were calculated for the four treatment groups (low, mid, and high dose plus controls). Because of the small group sizes and wide SDs for some variables, nonparametric tests were used. For each time point (baseline, interim, and final), the four groups were first compared using a Kruskal-Wallis test and, if differences were noted, each pair was further compared using the Dunn post hoc test. Combined "control and low-dose" versus "mid- and high-dose" groups were compared using the Mann-Whitney-Wilcoxon test. In comparing time points across ages, data were combined into a single longitudinal linear mixed model, using the same tests to compare the four groups and each pair. Another linear mixed model was used to compare the combined control and low-dose versus mid- and high-dose groups. In addition, multiple-comparison correction was applied. To quantify the longitudinal characteristics of the MRI biomarkers, we adopted a linear mixed model as previously reported (*44*). The relationship between WB and MS protein values was defined by Spearman's rank-order correlation. Resulting P values for all analyses were corrected for multiple comparisons and considered significant at $P < 0.05$.

Supplementary Materials

This PDF file includes:
Materials and Methods
Figs. S1 to S10
Tables S1 to S17
References (*72*–*78*)

Other Supplementary Material for this manuscript includes the following:
MDAR Reproducibility Checklist

View/request a protocol for this paper from *Bio-protocol*.

REFERENCES AND NOTES

1. D. Duan, N. Goemans, S. Takeda, E. Mercuri, A. Aartsma-Rus, Duchenne muscular dystrophy. *Nat. Rev. Dis. Primers.* **7**, 13 (2021).
2. M. Roberts, G. Dickson, The future of Duchenne muscular dystrophy gene therapy: Shrinking the dystrophin gene. *Curr. Opin. Mol. Ther.* **4**, 343–348 (2002).
3. D. J. Wells, A. Ferrer, K. E. Wells, Immunological hurdles in the path to gene therapy for Duchenne muscular dystrophy. *Expert Rev. Mol. Med.* **4**, 1–23 (2002).
4. D. Duan, Systemic AAV micro-dystrophin gene therapy for Duchenne muscular dystrophy. *Mol. Ther.* **26**, 2337–2356 (2018).
5. J. M. Crudele, J. S. Chamberlain, AAV-based gene therapies for the muscular dystrophies. *Hum. Mol. Genet.* **28**, R102–R107 (2019).
6. A. P. Monaco, C. J. Bertelson, S. Liechti-Gallati, H. Moser, L. M. Kunkel, An explanation for the phenotypic differences between patients bearing partial deletions of the DMD locus. *Genomics* **2**, 90–95 (1988).
7. B. Wang, J. Li, X. Xiao, Adeno-associated virus vector carrying human minidystrophin genes effectively ameliorates muscular dystrophy in mdx mouse model. *Proc. Natl. Acad. Sci. U.S.A.* **97**, 13714–13719 (2000).
8. S. Q. Harper, M. A. Hauser, C. DelloRusso, D. Duan, R. W. Crawford, S. F. Phelps, H. A. Harper, A. S. Robinson, J. F. Engelhardt, S. V. Brooks, J. S. Chamberlain, Modular flexibility of dystrophin: Implications for gene therapy of Duchenne muscular dystrophy. *Nat. Med.* **8**, 253–261 (2002).
9. J. R. Mendell, K. Campbell, L. Rodino-Klapac, Z. Sahenk, C. Shilling, S. Lewis, D. Bowles, S. Gray, C. Li, G. Galloway, V. Malik, B. Coley, K. R. Clark, J. Li, X. Xiao, J. Samulski, S. W. McPhee, R. J. Samulski, C. M. Walker, Dystrophin immunity in Duchenne's muscular dystrophy. *N. Engl. J. Med.* **363**, 1429–1437 (2010).
10. D. E. Bowles, S. W. McPhee, C. Li, S. J. Gray, J. J. Samulski, A. S. Camp, J. Li, B. Wang, P. E. Monahan, J. E. Rabinowitz, J. C. Grieger, L. Govindasamy, M. Agbandje-McKenna, X. Xiao, R. J. Samulski, Phase 1 gene therapy for Duchenne muscular dystrophy using a translational optimized AAV vector. *Mol. Ther.* **20**, 443–455 (2012).
11. J. N. Kornegay, The golden retriever model of Duchenne muscular dystrophy. *Skelet. Muscle* **7**, 9 (2017).
12. K. Yuasa, M. Yoshimura, N. Urasawa, S. Ohshima, J. M. Howell, A. Nakamura, T. Hijikata, Y. Miyagoe-Suzuki, S. Takeda, Injection of a recombinant AAV serotype 2 into canine skeletal muscles evokes strong immune responses against transgene products. *Gene Ther.* **14**, 1249–1260 (2007).
13. Z. Wang, J. M. Allen, S. R. Riddell, P. Gregorevic, R. Storb, S. J. Tapscott, J. S. Chamberlain, C. S. Kuhr, Immunity to adeno-associated virus-mediated gene transfer in a random-bred canine model of Duchenne muscular dystrophy. *Hum. Gene Ther.* **18**, 18–26 (2007).
14. Z. Wang, C. S. Kuhr, J. M. Allen, M. Blankinship, P. Gregorevic, J. S. Chamberlain, S. J. Tapscott, R. Storb, Sustained AAV-mediated dystrophin expression in a canine model of Duchenne muscular dystrophy with a brief course of immunosuppression. *Mol. Ther.* **15**, 1160–1166 (2007).
15. J. H. Shin, X. Pan, C. H. Hakim, H. T. Yang, Y. Yue, K. Zhang, R. L. Terjung, D. Duan, Microdystrophin ameliorates muscular dystrophy in the canine model of Duchenne muscular dystrophy. *Mol. Ther.* **21**, 750–757 (2013).
16. M. Z. Salva, C. L. Himeda, P. W. Tai, E. Nishiuchi, P. Gregorevic, J. M. Allen, E. E. Finn, Q. G. Nguyen, M. J. Blankinship, L. Meuse, J. S. Chamberlain, S. D. Hauschka, Design of tissue-specific regulatory cassettes for high-level rAAV-mediated expression in skeletal and cardiac muscle. *Mol. Ther.* **15**, 320–329 (2007).
17. J. N. Ramos, K. Hollinger, N. E. Bengtsson, J. M. Allen, S. D. Hauschka, J. S. Chamberlain, Development of novel micro-dystrophins with enhanced functionality. *Mol. Ther.* **27**, 623–635 (2019).
18. T. Koo, T. Okada, T. Athanasopoulos, H. Foster, S. Takeda, G. J. Dickson, Long-term functional adeno-associated virus-microdystrophin expression in the dystrophic CXMDj dog. *J. Gene Med.* **13**, 497–506 (2011).
19. M. Guilbaud, M. Devaux, C. Couzinié, J. Le Duff, A. Toromanoff, C. Vandamme, N. Jaulin, G. Gernoux, T. Larcher, P. Moullier, C. Le Guiner, O. Adjali, Five years of successful inducible transgene expression following locoregional adeno-associated virus delivery in nonhuman primates with no detectable immunity. *Hum. Gene Ther.* **30**, 802–813 (2019).
20. P. Gregorevic, M. J. Blankinship, J. M. Allen, J. S. Chamberlain, Systemic microdystrophin gene delivery improves skeletal muscle structure and function in old dystrophic mdx mice. *Mol. Ther.* **16**, 657–664 (2008).
21. B. Wang, J. Li, F. H. Fu, X. Xiao, Systemic human minidystrophin gene transfer improves functions and life span of dystrophin and dystrophin/utrophin-deficient mice. *J. Orthop. Res.* **27**, 421–426 (2009).
22. B. Bostick, J. H. Shin, Y. Yue, D. Duan, AAV-microdystrophin therapy improves cardiac performance in aged female mdx mice. *Mol. Ther.* **19**, 1826–1832 (2011).
23. Y. Yue, X. Pan, C. H. Hakim, K. Kodippili, K. Zhang, J. H. Shin, H. T. Yang, T. McDonald, D. Duan, Safe and bodywide muscle transduction in young adult Duchenne muscular dystrophy dogs with adeno-associated virus. *Hum. Mol. Genet.* **15**, 5880–5890 (2015).
24. C. Le Guiner, L. Servais, M. Montus, T. Larcher, B. Fraysse, S. Moullec, M. Allais, V. François, M. Dutilleul, A. Malerba, T. Koo, J. L. Thibaut, B. Matot, M. Devaux, J. Le Duff, J. Y. Deschamps, I. Barthelemy, S. Blot, I. Testault, K. Wahbi, S. Ederhy, S. Martin, P. Veron, C. Georger, T. Athanasopoulos, C. Masurier, F. Mingozzi, P. Carlier, B. Gjata, J. Y. Hogrel, O. Adjali, F. Mavilio, T. Voit, P. Moullier, G. Dickson, Long-term microdystrophin gene therapy is

effective in a canine model of Duchenne muscular dystrophy. *Nat. Commun.* **8**, 16105 (2017).

25. C. H. Hakim, N. B. Wasala, X. Pan, K. Kodippili, Y. Yue, K. Zhang, G. Yao, B. Haffner, S. X. Duan, J. Ramos, J. S. Schneider, N. N. Yang, J. S. Chamberlain, D. Duan, A five-repeat microdystrophin gene ameliorated dystrophic phenotype in the severe DBA/2J-mdx model of Duchenne muscular dystrophy. *Mol. Ther. Methods Clin. Dev.* **6**, 216–230 (2017).
26. J. N. Kornegay, J. Li, J. R. Bogan, D. J. Bogan, C. Chen, H. Zheng, B. Wang, C. Qiao, J. F. Howard Jr., X. Xiao, Widespread muscle expression of an AAV9 human mini-dystrophin vector after intravenous injection in neonatal dystrophin-deficient dogs. *Mol. Ther.* **18**, 1501–1508 (2010).
27. A. Ferrer, K. E. Wells, D. J. Wells, Immune responses to dystrophin: Implications for gene therapy of Duchenne muscular dystrophy. *Gene Ther.* **7**, 1439–1446 (2000).
28. J. N. Kornegay, J. M. Peterson, D. J. Bogan, W. Kline, J. R. Bogan, J. L. Dow, Z. Fan, J. Wang, M. Ahn, H. Zhu, M. Styner, D. C. Guttridge, NBD delivery improves the disease phenotype of the golden retriever model of Duchenne muscular dystrophy. *Skelet. Muscle* **4**, 18 (2014).
29. J. N. Kornegay, J. R. Bogan, D. J. Bogan, M. K. Childers, J. Li, P. Nghiem, D. A. Detwiler, C. A. Larsen, R. W. Grange, R. K. Bhavaraju-Sanka, S. Tou, B. P. Keene, J. F. Howard Jr., J. Wang, Z. Fan, S. J. Schatzberg, M. A. Styner, K. M. Flanigan, X. Xiao, E. P. Hoffman, Canine models of Duchenne muscular dystrophy and their use in therapeutic strategies. *Mamm. Genome* **23**, 85–108 (2012).
30. C. Zincarelli, S. Soltys, G. Rengo, J. E. Rabinowitz, Analysis of AAV serotypes 1-9 mediated gene expression and tropism in mice after systemic injection. *Mol. Ther.* **16**, 1073–1080 (2008).
31. Y. Yue, A. Ghosh, C. Long, B. Bostick, B. F. Smith, J. N. Kornegay, D. Duan, A single intravenous injection of adeno-associated virus serotype-9 leads to whole body skeletal muscle transduction in dogs. *Mol. Ther.* **16**, 1944–1952 (2008).
32. V. Arechavala-Gomeza, M. Kinali, L. Feng, M. Guglieri, G. Edge, M. Main, D. Hunt, J. Lehovsky, V. Straub, K. Bushby, C. A. Sewry, J. E. Morgan, F. Muntoni, Revertant fibres and dystrophin traces in Duchenne muscular dystrophy: Implication for clinical trials. *Neuromuscul. Disord.* **20**, 295–301 (2010).
33. J. N. Kornegay, D. D. Cundiff, D. J. Bogan, J. R. Bogan, C. S. Okamura, The cranial sartorius muscle undergoes true hypertrophy in dogs with golden retriever muscular dystrophy. *Neuromuscul. Disord.* **13**, 493–500 (2003).
34. L. T. Thanh, T. M. Nguyen, T. R. Helliwell, G. E. Morris, Characterization of revertant muscle fibers in Duchenne muscular dystrophy, using exon-specific monoclonal antibodies against dystrophin. *Am. J. Hum. Genet.* **56**, 725–731 (1995).
35. Y. Lai, G. D. Thomas, Y. Yue, H. T. Yang, D. Li, C. Long, L. Judge, B. Bostick, J. S. Chamberlain, R. L. Terjung, D. Duan, Dystrophins carrying spectrin-like repeats 16 and 17 anchor nNOS to the sarcolemma and enhance exercise performance in a mouse model of muscular dystrophy. *J. Clin. Invest.* **119**, 624–635 (2009).
36. Y. M. Kobayashi, E. P. Rader, R. W. Crawford, N. K. Iyengar, D. R. Thedens, J. A. Faulkner, S. V. Parikh, R. M. Weiss, J. S. Chamberlain, S. A. Moore, K. P. Campbell, Sarcolemma-localized nNOS is required to maintain activity after mild exercise. *Nature* **456**, 511–515 (2008).
37. K. J. Brown, R. Marathi, A. A. Fiorillo, E. F. Ciccimaro, S. Sharma, D. S. Rowlands, S. Rayavarapu, K. Nagaraju, E. P. Hoffman, Y. Hathout, Accurate quantitation of dystrophin protein in human skeletal muscle using mass spectrometry. *J. Bioanal. Biomed.* **Suppl 7**, 001 (2012).
38. V. Farrokhi, J. Walsh, J. Palandra, J. Brodfuehrer, T. Caiazzo, J. Owens, M. Binks, S. Neelakantan, F. Yong, P. Dua, C. Le Guiner, H. Neubert, Dystrophin and mini-dystrophin quantification by mass spectrometry in skeletal muscle for gene therapy development in Duchenne muscular dystrophy. *Gene Ther.* **29**, 608–615 (2022).
39. M. C. Vila, J. S. Novak, M. Benny Klimek, N. Li, M. Morales, A. G. Fritz, K. Edwards, J. F. Boehler, M. W. Hogarth, T. B. Kinder, A. Zhang, D. Mazala, A. A. Fiorillo, B. Douglas, Y. W. Chen, J. van den Anker, Q. L. Lu, Y. Hathout, E. P. Hoffman, T. A. Partridge, K. Nagaraju, Morpholino-induced exon skipping stimulates cell-mediated and humoral responses to dystrophin in mdx mice. *J. Pathol.* **248**, 339–351 (2019).
40. M. K. Childers, C. S. Okamura, D. J. Bogan, J. R. Bogan, M. J. Sullivan, J. N. Kornegay, Myofiber injury and regeneration in a canine homologue of Duchenne muscular dystrophy. *Am. J. Phys. Med. Rehabil.* **80**, 175–181 (2001).
41. B. A. Valentine, B. J. Cooper, J. F. Cummings, A. de Lahunta, Canine X-linked muscular dystrophy: Morphologic lesions. *J. Neurol. Sci.* **97**, 1–23 (1990).
42. J. F. Wang, J. Forst, S. Schröder, J. M. Schröder, Correlation of muscle fiber type measurements with clinical and molecular genetic data in Duchenne muscular dystrophy. *Neuromuscul. Disord.* **9**, 150–158 (1999).
43. A. M. Barnard, R. J. Willcocks, E. L. Finanger, M. J. Daniels, W. T. Triplett, W. D. Rooney, D. J. Lott, S. C. Forbes, D. J. Wang, C. R. Senesac, A. T. Harrington, R. S. Finkel, B. S. Russman, B. J. Byrne, G. I. Tennekoon, G. A. Walter, H. L. Sweeney, K. Vandenborne, Skeletal muscle magnetic resonance biomarkers correlate with function and sentinel events in Duchenne muscular dystrophy. *PLOS ONE* **13**, e0194283 (2018).
44. Z. Fan, J. Wang, M. Ahn, Y. Shiloh-Malawsky, N. Chahin, S. Elmore, C. R. Bagnell Jr., K. Wilber, H. An, W. Lin, H. Zhu, M. Styner, J. N. Kornegay, Characteristics of magnetic resonance imaging biomarkers in a natural history study of golden retriever muscular dystrophy. *Neuromuscul. Disord.* **24**, 178–191 (2014).
45. J. N. Kornegay, D. J. Bogan, J. R. Bogan, M. K. Childers, D. D. Cundiff, G. F. Petroski, R. O. Schueler, Contraction force generated by tarsal joint flexion and extension in dogs with golden retriever muscular dystrophy. *J. Neurol. Sci.* **166**, 115–121 (1999).
46. A. R. Acosta, E. Van Wie, W. B. Stoughton, A. K. Bettis, H. H. Barnett, N. R. LaBrie, C. J. Balog-Alvarez, P. P. Nghiem, K. J. Cummings, J. N. Kornegay, Use of the six-minute walk test to characterize golden retriever muscular dystrophy. *Neuromuscul. Disord.* **26**, 865–872 (2016).
47. C. J. Tegeler, R. W. Grange, D. J. Bogan, C. D. Markert, D. Case, J. N. Kornegay, M. K. Childers, Eccentric contractions induce rapid isometric torque drop in dystrophin-deficient dogs. *Muscle Nerve* ***42***, 130–132 (2010).
48. J. M. K. Liu, C. S. Okamura, D. J. Bogan, J. R. Bogan, M. K. Childers, J. N. Kornegay, Effects of prednisone in canine muscular dystrophy. *Muscle Nerve* **30**, 767–773 (2004).
49. D. J. Birnkrant, K. Bushby, C. M. Bann, B. A. Alman, S. D. Apkon, A. Blackwell, L. E. Case, L. Cripe, S. Hadjiyannakis, A. K. Olson, D. W. Sheehan, J. Bolen, D. R. Weber, L. M. Ward; DMD Care Considerations Working Group, Diagnosis and management of Duchenne muscular dystrophy, part 2: Respiratory, cardiac, bone health, and orthopaedic management. *Lancet Neurol.* **17**, 347–361 (2018).
50. J. C. DeVanna, J. N. Kornegay, D. J. Bogan, J. R. Bogan, J. L. Dow, E. C. Hawkins, Respiratory dysfunction in unsedated dogs with golden retriever muscular dystrophy. *Neuromuscul. Disord.* **24**, 63–73 (2014).
51. E. C. Hawkins, A. K. Bettis, J. N. Kornegay, Expiratory dysfunction in young dogs with golden retriever muscular dystrophy. *Neuromuscul. Disord.* **30**, 930–937 (2020).
52. L.-J. Guo, J. H. Soslow, A. K. Bettis, K. J. Cummings, M. W. Lenox, M. W. Miller, J. N. Kornegay, C. F. Spurney, Natural history of cardiomyopathy in adult dogs with golden retriever muscular dystrophy. *J. Am. Heart Assoc.* **8**, e012443 (2019).
53. C. Veropalumbo, E. Del Giudice, G. Esposito, S. Maddaluno, L. Ruggiero, P. Vajro, Amino-transferases and muscular diseases: A disregarded lesson. Case reports and review of the literature. *J. Paediatr. Child Health* **48**, 886–890 (2012).
54. J. P. Aston, H. M. Kingston, I. Ramasamy, E. G. Walters, D. Stansbie, Plasma pyruvate kinase and creatine kinase activity in Becker muscular dystrophy. *J. Neurol. Sci.* **65**, 307–314 (1984).
55. B. D. Rodgers, Y. Bishaw, D. Kagel, J. N. Ramos, J. W. Maricelli, Micro-dystrophin gene therapy partially enhances exercise capacity in older adult mdx mice. *Mol. Ther. Methods Clin. Dev.* **17**, 122–132 (2019).
56. B. A. Valentine, J. T. Blue, S. M. Shelley, B. J. Cooper, Increased serum alanine amino-transferase activity associated with muscle necrosis in the dog. *J. Vet. Intern. Med.* **4**, 140–143 (1990).
57. I. Barthélémy, A. Uriarte, C. Drougard, Y. Unterfinger, J. L. Thibaud, S. Blot, Effects of an immunosuppressive treatment in the GRMD dog model of Duchenne muscular dystrophy. *PLOS ONE* **7**, e48478 (2012).
58. J. Manning, D. O'Malley, What has the mdx mouse model of Duchenne muscular dystrophy contributed to our understanding of this disease? *J. Muscle Res. Cell Motil.* **36**, 155–167 (2015).
59. V. R. Arruda, H. H. Stedman, V. Haurigot, G. Buchlis, S. Baila, P. Favaro, Y. Chen, H. G. Franck, S. Zhou, J. F. Wright, L. B. Couto, H. Jiang, G. F. Pierce, D. A. Bellinger, F. Mingozzi, T. C. Nichols, K. A. High, Peripheral transvenular delivery of adeno-associated viral vectors to skeletal muscle as a novel therapy for hemophilia B. *Blood* **115**, 4678–4688 (2010).
60. R. Storb, E. D. Thomas, Graft-versus-host disease in dog and man: The Seattle experience. *Immunol. Rev.* **88**, 215–238 (1985).
61. K. M. Flanigan, K. Campbell, L. Viollet, W. Wang, A. M. Gomez, C. M. Walker, J. R. Mendell, Anti-dystrophin T cell responses in Duchenne muscular dystrophy: Prevalence and a glucocorticoid treatment effect. *Hum. Gene Ther.* **24**, 797–806 (2013).
62. D. Cheeran, S. Khan, R. Khera, A. Bhatt, S. Garg, J. L. Grodin, R. Morlend, F. G. Araj, A. A. Amin, J. T. Thibodeau, S. Das, M. H. Drazner, P. P. A. Mammen, Predictors of death in adults with Duchenne muscular dystrophy-associated cardiomyopathy. *J. Am. Heart Assoc.* **6**, e006340 (2017).
63. H. Fang, N. C. Lai, M. H. Gao, A. Miyanohara, D. M. Roth, T. Tang, H. K. Hammond, Comparison of adeno-associated virus serotypes and delivery methods for cardiac gene transfer. Version 2. *Hum. Gene Ther. Methods.* **23**, 234–241 (2012).
64. N. Elangkovan, G. Dickson, Gene therapy for Duchenne muscular dystrophy. *J. Neuromuscul. Dis.* **8**, S303–S316 (2021).
65. Solid Biosciences provides update regarding SGT-001 phase I/II clinical hold on IGNITE DMD (2020); www.solidbio.com/about/media/press-releases/solid-biosciences-provides-update-regarding-sgt-001-phase-i-ii-clinical-hold-on-ignite-dmd.

66. J. R. Mendell, S. A. Al-Zaidy, L. R. Rodino-Klapac, K. Goodspeed, S. J. Gray, C. N. Kay, S. L. Boye, S. E. Boye, L. A. George, S. Salabarria, M. Corti, B. J. Byrne, J. P. Tremblay, Current clinical applications of in vivo gene therapy with AAVs. *Mol. Ther.* **29**, 464–488 (2021).
67. J. R. Mendell, P. B. Shieh, Z. Sahenk, K. J. Lehman, L. P. Lowes, N. F. Reash, M. A. Iammarino, L. N. Alfano, B. Powers, J. D. Woods, C. L. Skura, H. C. Mao, L. A. Staudt, R. A. Potter, D. A. Griffin, S. Lewis, L. Hu, S. Upadhyay, T. Singh, L. R. Rodino-Klapac, A phase 2 clinical trial evaluating the safety and efficacy of delandistrogene moxeparvovec (SRP-9001) in patients with Duchenne muscular dystrophy. Presented at the 2022 Muscular Dystrophy Association (MDA) Conference, Nashville, TN, USA, 13–16 March 2022; https://investorrelations.sarepta.com/static-files/56830179-3bb0-4796-8fdc-1b43c989a899.
68. R. J. Butterfield, P. B. Shieh, F. Yong, M. Binks, T. G. McDonnell, K. A. Ryan, M. Delnomdedieu, B. A. Belluscio, S. Neelakantan, D. I. Levy, P. F. Schwartz, E. C. Smith, Results of one year follow-up after treatment with fordadistrogene movaparvovec (PF-06939926) for Duchenne muscular dystrophy (DMD) in a phase 1b, open-label study. *Mol. Ther.* **30**, 4–5 (2022).
69. A. K. Zaiss, M. J. Cotter, L. R. White, S. A. Clark, N. C. Wong, V. M. Holers, J. S. Bartlett, D. A. Muruve, Complement is an essential component of the immune response to adeno-associated virus vectors. *J. Virol.* **82**, 2727–2740 (2008).
70. C. G. Bonnemann, B. A. Belluscio, S. Braun, C. Morris, T. Singh, F. Muntoni, A collaborative analysis by clinical trial sponsors and academic experts of anti-transgene SAEs in studies of gene therapy for DMD. *Mol. Ther.* **30 (suppl. 1)**, 3 (2022).
71. J. N. Kornegay, J. R. Bogan, D. J. Bogan, M. K. Childers, R. W. Grange, Golden retriever muscular dystrophy (GRMD): Developing and maintaining a colony and physiological functional measurements. in *Muscle Gene Therapy: Methods and Protocols*, D. Duan, Ed. (Humana Press, 2011), Methods in Molecular Biology, vol. 709, pp. 105–123.
72. R. J. Bartlett, N. J. Winand, S. L. Secore, J. T. Singer, S. Fletcher, S. Wilton, D. J. Bogan, J. R. Metcalf-Bogan, W. T. Bartlett, J. M. Howell, B. J. Cooper, J. N. Kornegay, Mutation segregation and rapid carrier detection of X-linked muscular dystrophy in dogs. *Am. J. Vet. Res.* **57**, 650–654 (1996).
73. G. J. Patronek, D. J. Waters, L. T. Glickman, Comparative longevity of pet dogs and humans: Implications for gerontology research. *J. Gerontol. A Biol. Sci. Med. Sci.* **52**, B171–B178 (1997).
74. C. M. McDonald, R. T. Abresch, G. T. Carter, W. M. Fowler Jr., E. R. Johnson, D. D. Kilmer, B. J. Sigford, Profiles of neuromuscular diseases. Duchenne muscular dystrophy. *Am. J. Phys. Med. Rehabil.* **74**(5 Suppl), S70–S92 (1995).
75. V. Haurigot, F. Mingozzi, G. Buchlis, D. J. Hui, Y. Chen, E. Basner-Tschakarjan, V. R. Arruda, A. Radu, H. G. Franck, J. F. Wright, S. Zhou, H. H. Stedman, D. A. Bellinger, T. C. Nichols, K. A. High, Safety of AAV factor IX peripheral transvenular gene delivery to muscle in hemophilia B dogs. *Mol. Ther.* **18**, 1318–1329 (2010).
76. L. H. Vandenberghe, R. Xiao, M. Lock, J. Lin, M. Korn, J. M. Wilson, Efficient serotype-dependent release of functional vector into the culture medium during adeno-associated virus manufacturing. *Hum. Gene Ther.* **21**, 1251–1257 (2010).
77. H. Meng, P. M. Janssen, R. W. Grange, L. Yang, A. H. Beggs, L. C. Swanson, S. A. Cossette, A. Frase, M. K. Childers, H. Granzier, E. Gussoni, M. W. Lawlor, Tissue triage and freezing for models of skeletal muscle disease. *J. Vis. Exp.* , 51586 (2014).
78. K. Matsumura, F. M. Tomé, V. Ionasescu, J. M. Ervasti, R. D. Anderson, N. B. Romero, D. Simon, D. Récan, J. C. Kaplan, M. Fardeau, Deficiency of dystrophin-associated proteins in Duchenne muscular dystrophy patients lacking COOH-terminal domains of dystrophin. *J. Clin. Invest.* **92**, 866–871 (1993).

Acknowledgments: We thank the veterinarians and technical staff of the Texas A&M Comparative Medicine Program for the care provided to the dogs in this study. Q. Nguyen and X. Chen are acknowledged for their efforts in developing the CK8e muscle-specific expression cassette. **Funding:** This research was supported by a grant from Solid Biosciences Inc. to J.N.K. and a U.S. Department of Defense (DOD), Congressionally Directed Medical Research Programs (CDMRP), Duchenne Muscular Dystrophy Research Program (DMDRP) grant (MD120087) to B.J.B. Additional funding for contributions to the study was provided by the NIH to J.S.C. (R01 AR40864) and D.D. (NS-90634). M.J.S. received equity funding from Solid Biosciences. **Author contributions:** S.M.B., M.W.L., J.P.G., C.A.M., J.S.S., M.C., B.J.B., and J.N.K. participated in the study design. S.M.B. supervised the day-to-day conduct of the study. S.M.B., J.P.G., M.W.L., M.J.S., C.S., A.K.B., C.J.B.-A., H.M., M.J.B., B.A.F., K.E.C., and M.C. collected and organized the data. P.P.N. and J.N.K. performed and interpreted skeletal muscle physiology tests. L.-J.G. performed and interpreted cardiac tests. E.C.H. performed and interpreted respiratory tests. J.M.C. and J.S.C. supervised and interpreted ELISPOT assays. J.C.P. and M.A.S. conducted and oversaw the MRI analysis. H.M., M.J.B., and B.A.F. performed the histologic and immunoblot studies. M.W.L. oversaw and interpreted the histopathological and immunoblot studies. K.J.B. supervised and interpreted the MS studies. D.G. and T.J.C. supervised the vector biodistribution studies. M.A. conducted the statistical analysis. A.K.B. supervised or conducted the anesthesia and 6MWT studies. K.E.C. performed the biodistribution studies. M.C. contributed to immune assays. S.D.H. designed the CK8e muscle-specific expression cassette. J.S.C. designed the AAV9-CK8e-μDys5 vector. D.D. and X.P. designed and cloned the canine version of the AAV9-CK8e-μDys5 vector. B.J.B. and J.N.K. secured funding for the project. J.N.K. wrote the initial draft of the manuscript. All authors reviewed the manuscript. **Competing interests:** D.D. and J.S.C. are members of the scientific advisory board, equity holders, and inventors on patents licensed to Solid Biosciences Inc. D.D. is an inventor on related intellectual property owned by the University of Missouri: Synthetic mini/micro-dystrophin genes to restore nNOS to the sarcolemma, U.S. patent number 7,892,824. J.S.C. and S.D.H. are inventors on related intellectual property owned by the University of Washington, including (i) Compositions and methods for systemic nucleic acid sequence delivery, U.S. patent no. 7,655,467; (ii) Micro-dystrophins and related methods of use, U.S. patent number 10,479,821; and (iii) Regulatory cassettes for muscle-specific gene expression, U.S. patent provisional application 63/173,295. The Duan, Chamberlain, Lawlor, and Kornegay laboratories have received research support from Solid Biosciences Inc. M.J.S., K.J.B., D.G., J.P.G., C.A.M., and J.S.S. are or were employees of Solid Biosciences Inc. J.N.K. was a paid consultant for Solid Biosciences Inc. P.P.N. is a paid consultant for Agada Biosciences. **Data and materials availability:** All data associated with this study are present in the paper or the Supplementary Materials. The CK8e muscle-specific promoter used in this study was made available from the University of Washington and J.S.C./S.D.H. under a material agreement with the University of Missouri-Columbia and D.D. The canine version of the CK8e-μDys5 vector was subsequently cloned by the Duan laboratory.

Submitted 18 January 2022
Accepted 9 December 2022
Published 4 January 2023
10.1126/scitranslmed.abo1815